OPEN

Disruption of the Extracellular Matrix Progressively Impairs Central Nervous System Vascular Maturation Downstream of β-Catenin Signaling

Lasse D. Jensen,* Belma Hot,* Daniel Ramsköld, Raoul F.V. Germano, Chika Yokota, Sarantis Giatrellis, Volker M. Lauschke, Dirk Hubmacher, Minerva X. Li, Mike Hupe, Thomas D. Arnold, Rickard Sandberg, Jonas Frisén, Marta Trusohamn, Agnieszka Martowicz, Joanna Wisniewska-Kruk, Daniel Nyqvist, Ralf H. Adams, Suneel S. Apte, Benoit Vanhollebeke, Jan M. Stenman, Julianna Kele

Objective—The Wnt/β-catenin pathway orchestrates development of the blood-brain barrier, but the downstream mechanisms involved at different developmental windows and in different central nervous system (CNS) tissues have remained elusive.

Approach and Results—Here, we create a new mouse model allowing spatiotemporal investigations of Wnt/β-catenin signaling by induced overexpression of Axin1, an inhibitor of β-catenin signaling, specifically in endothelial cells (*Axin1*$^{iEC-OE}$). AOE (Axin1 overexpression) in *Axin1*$^{iEC-OE}$ mice at stages following the initial vascular invasion of the CNS did not impair angiogenesis but led to premature vascular regression followed by progressive dilation and inhibition of vascular maturation resulting in forebrain-specific hemorrhage 4 days post-AOE. Analysis of the temporal Wnt/β-catenin driven CNS vascular development in zebrafish also suggested that *Axin1*$^{iEC-OE}$ led to CNS vascular regression and impaired maturation but not inhibition of ongoing angiogenesis within the CNS. Transcriptomic profiling of isolated, β-catenin signaling-deficient endothelial cells during early blood-brain barrier–development (E11.5) revealed ECM (extracellular matrix) proteins as one of the most severely deregulated clusters. Among the 20 genes constituting the forebrain endothelial cell-specific response signature, 8 (*Adamtsl2*, *Apod*, *Ctsw*, *Htra3*, *Pglyrp1*, *Spock2*, *Ttyh2*, and *Wfdc1*) encoded bona fide ECM proteins. This specific β-catenin-responsive ECM signature was also repressed in *Axin1*$^{iEC-OE}$ and endothelial cell-specific β-catenin–knockout mice (*Ctnnb*1-KO^{iEC}) during initial blood-brain barrier maturation (E14.5), consistent with an important role of Wnt/β-catenin signaling in orchestrating the development of the forebrain vascular ECM.

Conclusions—These results suggest a novel mechanism of establishing a CNS endothelium-specific ECM signature downstream of Wnt-β-catenin that impact spatiotemporally on blood-brain barrier differentiation during forebrain vessel development.

Visual Overview—An online visual overview is available for this article. **(*Arterioscler Thromb Vasc Biol*. 2019;39:1432-1447. DOI: 10.1161/ATVBAHA.119.312388.)**

Key Words: basement membrane ■ blood-brain barrier ■ central nervous system ■ embryonic development ■ endothelial cells ■ extracellular matrix ■ vasculature

The brain vasculature and the blood-brain barrier (BBB) are critical for normal central nervous system (CNS) development and homeostasis. The integrity of the BBB is a prerequisite for appropriate neural function and is compromised in a wide variety of neurological diseases ranging from Alzheimer disease to neurological cancers.[1] To achieve barrier function, endothelial cells (ECs) in the brain are joined with continuous tight junctions, tightly covered with vascular mural cells and astrocytic end-feet and express a unique selection of transporters and plasma membrane pumps to facilitate uptake of essential

Received on: June 7, 2018; final version accepted on: April 24, 2019.

From the Department of Medical and Health Sciences, Linköpings Universitet, Linköping, Sweden (L.D.J.); Department of Physiology and Pharmacology (B.H., V.M.L., J.K.), Department of Medicine, Solna (D.R.), Department of Medical Biochemistry and Biophysics (M.T., A.M., J.W.-K., D.N.), Department of Cell and Molecular Biology (D.R., S.G., R.S., J.F.), Karolinska Institutet, Stockholm, Sweden; Ludwig Institute for Cancer Research Ltd, Stockholm, Sweden (B.H., D.R., C.Y., M.X.L., M.H., R.S., J.M.S., J.K.); Laboratory of Neurovascular Signaling, Department of Molecular Biology, Université libre de Bruxelles, Belgium (R.F.V.G., B.V.); Orthopaedic Research Laboratories, Department of Orthopaedics, Icahn School of Medicine at Mount Sinai, New York, NY (D.H.); Department of Clinical Sciences, Lunds Universitet, Sweden (M.X.L.); Developmental Biochemistry, Theodor Boveri Institute (Biocenter), University of Wuerzburg, Germany (M.H.); Department of Pediatrics, University of California, San Francisco (T.D.A.); Department of Tissue Morphogenesis Max-Planck-Institute for Molecular Biomedicine, University of Münster, Faculty of Medicine, Germany (R.H.A.); Department of Biomedical Engineering, Cleveland Clinic Lerner Research Institute, Cleveland Clinic Foundation (S.S.A.); Walloon Excellence in Life Sciences and Biotechnology (WELBIO), Belgium (B.V.); and Department of Biochemistry and Biophysics, Stockholm University, Sweden (C.Y.).

*L.D. Jensen and B. Hot are joint first authors.

The online-only Data Supplement is available with this article at https://www.ahajournals.org/doi/suppl/10.1161/ATVBAHA.119.312388.

Correspondence to Julianna Kele, PhD, Department of Physiology and Pharmacology, Karolinska Institutet, Solnavägen 9, SE-177, Sweden. Email julianna.kele@ki.se

Nonstandard Abbreviations and Acronyms	
AOE	Axin1 overexpression
BBB	blood-brain barrier
Cldn5	claudin5
CNS	central nervous system
CtAs	central arteries
ECs	endothelial cells
ECM	extracellular matrix
Fzd4	Frizzled 4
MGE	medial ganglionic eminence
MMPs	matrix metalloproteinases
PVP	perivascular plexus
TRAP	translating ribosome affinity purification

nutrients such as glucose.[2] At the same time, this specialized vasculature actively shields the CNS from toxic insults. A second mechanism of barrier formation is the deposition of a unique basement membrane by ECs in concert with mural cells and astrocytes that comprises an intricate multicomponent 3-dimensional network of ECM (extracellular matrix) glycoproteins.[3]

Brain development depends on the delivery of oxygen and nutrients through angiogenic expansion of vascular networks originating outside the CNS. During mouse embryonic development, at embryonic day (E)7.5-E8.5, mesoderm-derived angioblasts, initially form a perineural vascular plexus.[4,5] Subsequently, they invade the brain radially at E9.5 in a precise spatiotemporal manner through angiogenic sprouting and form the perivascular plexus (PVP). During these developmental stages, an orchestrated interplay of cellular and noncellular molecular cues locally instructs CNS microvascular ECs to acquire their unique capability to form the BBB.[2] The Wnt/β-catenin pathway is as a key player in the formation, differentiation,[6–8] integrity,[9] and maintenance[10–12] of CNS vasculature. As such, EC-specific ablation of β-catenin results in severe hemorrhage observed throughout the CNS.[6] β-catenin has a dual role as a structural component of cell-cell junctions and as a key transducer of signaling by Wnt ligands.[13,14] In the CNS endothelium Axin1 is an important modulator of Wnt-signaling activity by regulating cytoplasmic β-catenin stability and lowering the pool of β-catenin available for entry into the nucleus, inhibiting β-catenin–mediated transcription.[10,15] The Wnt-family ligands involved in CNS vascular development and BBB formation include Wnt-7a/-7b[6,8] and Norrin[10,16,17] acting through the Frizzled 4 receptor (encoded by Fzd4),[10,16–18] low-density lipoprotein receptor-related protein 5/6 (encoded by Lrp5/6) coreceptors,[9] and the Tetraspanin-12 (encoded by Tspan12,Tm4sf12),[19] adhesion G-protein–coupled receptor 124 (encoded by Gpr124, Tem5),[20–23] and reversion-inducing cysteine-rich protein with Kazal motifs (encoded by Reck)[23–25] coactivators.

Development and maintenance of the BBB-associated ECM also involve MMPs (matrix metalloproteinases), including MMP-2, MMP-9, and MMP-12, whose upregulation is implicated in various brain disorders, including traumatic brain injury,[26] stroke,[27] and Alzheimer disease.[1] Furthermore, loss of the synthesis or impaired secretion of ECM proteins, such as Laminin α2, and α-dystroglycan[27,28] lead to disrupted BBB functions during brain development providing further evidence for the importance of the ECM in BBB organization and stability. As the role of Wnt-β-catenin signaling in BBB formation has mainly been studied in the context of intracellular signaling in ECs, effects on extracellular processes important for BBB formation such as ECM development and maintenance during development are poorly understood.

A better understanding of the Wnt-regulated molecular and cellular mechanism(s) are achieved by identifying the Wnt downstream target genes. Previous efforts towards this goal, including our previously reported Wnt-signaling-deficient mouse models,[6] however, exhibit severe CNS vascular phenotypes, leading to extensive brain dysfunction and activation of a host of pathological signaling cascades in both EC and other BBB-cells already at early developmental stages. Such severe models are, therefore, poor models for identifying Wnt-specific downstream target genes. For example, in the mouse model in which Wnt7a/b are ablated, almost no ECs invade the CNS parenchyma and severe hemorrhaging is observed already at embryonic day (E)11.5.[6] Therefore, a mouse model that allows conditional and cell-autonomous inhibition, but not complete blockade, of the Wnt-signaling pathway and at the same time labels the manipulated cells for easy identification both in vitro and in vivo, is needed to allow CNS vascular formation. Such a model would specifically inhibit BBB development, maturation, and maintenance. To achieve this, we generated a new transgenic mouse line that allows inducible Axin1 overexpression specifically in ECs (*Axin1*$^{iEC-OE}$) at different embryonic stages. This allowed us to define the spatiotemporal role of Wnt/β-catenin signaling during CNS vascular development and BBB formation. By using gene expression profiling of mouse ECs from various tissues and stages of embryonic development, we identified ECM remodeling as the main brain-specific process regulated by reduced Wnt/β-catenin signaling in forebrain ECs during early pathological vascular remodeling. This suggests that Wnt-β-catenin signaling regulates BBB-differentiation at least, in part, through establishing a CNS vasculature-specific ECM signature during development.

Materials and Methods

The data that support the findings of this study are available from the corresponding author upon reasonable request.

Statistical Analysis

For the mouse data, no significant deviations from normality were detected using the Kolmogorov-Smirnov test with Dallal-Wilkinson-Lillie for approximation at a threshold of $\alpha<0.05$, and 2-tailed heteroscedastic *t* tests with Welch correction for unequal variance between groups was applied using Prism 6 (GraphPad Software) if not stated differently. For formulas and details on RNA sequencing data, please see below Sample Processing, RNA Sequencing, and Statistical analysis section. In brief, for differential expression testing, we used a similar test as previously described.[29] False discovery rates were calculated by the Benjamini-Hochberg method. Genes with <5% false discovery rate were considered differentially expressed. For the E14.5 *Axin1*$^{iEC-OE}$ (Gene Expression Omnibus entry: GSE66848) and Ctnnb1-KO^{iEC} samples[30], we applied a <5% false discovery rate cutoff to the DESeq *P* values. These samples were prepared according to endothelial-specific translating ribosome affinity purification (TRAP) sequencing.[31]

For the zebrafish analysis and analysis of Cldn5 (claudin5) expression (Figure IV in the online-only Data Supplement) the data did not pass the normality test and differences between groups were, therefore, evaluated using a nonparametric Mann-Whitney test (please see below zebrafish manipulations, imaging, and statistical analysis).

Mouse Strains and Genotyping

Mouse strains are summarized in the Major Resources Tables (Table I in the online-only Data Supplement). Briefly, generation of *Cdh5CreERT2*,[32] *Flk1Cre*,[33] *Ctnnb1*$^{flox(ex2-6)/-}$,[6,34] *mCherryTRAP*,[30,31] the Wnt-reporter mouse strain: *TCF/Lef:H2B-GFP*[35] (Jackson Laboratory, stock no. 013752[35]) and *Adamtsl2*$^{-/-}$ or *Adamtsl2*$^{+/-}$[36] mice were described previously. *R26Axin1IL* (AOE [Axin1 overexpressing] mice) were generated for this study as described in the paragraph below. Vascular endothelium-specific and inducible AOE (*Axin1*$^{iEC-OE}$) embryos were generated by breeding male *Tg(Cdh5-cre/ERT2)1Rha (Cdh5-CreERT2*$^{+/-}$*)*[32] mice with *R26Axin1IL* females and were kept on a CD1 background. *Ctnnb1-KO*^{iEC} embryos resulted from intercrosses between Chd5-CreERT2$^{+/-}$[32] male and β-catenin *lox-P* flanked (floxed) *β-catenin*$^{flox/flox}$ (floxed *Ctnnb1*)[31] female mice and were maintained on a C57BL/6J background.

Inducible EC-specific TRAP[30,31] was performed by initially crossing male *Cdh5CreERT2*$^{+/-}$[32] with female *Gt(ROSA)26Sor-mCherry-Rpl10a* (*mCherryTRAP*$^{+/+}$)[30,31] mice to activate the mCherry transgene in vascular endothelium: the stop cassette (tpA: 3 SV40 polyAs) is deleted and the ubiquitous enhancer/promoter (CAGGS) drives expression of mCherry-tagged Rpl10a in the presence of Cre recombinase. To generate endothelial-specific AOE or Ctnnb1 knockout TRAP animals, we crossed male *Cdh5CreERT2*$^{+/-}$*;mCherryTRAP*$^{+/-}$ with female *R26Axin1IL*^{Homozygous} mice or a floxed Ctnnb1 allele was crossed into the *Cdh5CreERT2;mCherryTRAP* mouse line, and then, translated and transcribed RNAs from Ctnnb1-KO or AOE embryo forebrains were isolated and subjected to RNA-seq. RNA-seq data from *Axin1*$^{+/+}$*;Cdh5CreERT2;mCherryTRAP* or *Ctnnb1*$^{+/+}$*;Cdh5CreERT2;mCherryTRAP* embryos were used as control (for details see TRAP-Seq and TRAP-Seq of *β-catenin/Ctnnb1-KO*[30,31]).

Crosses between these strains as indicated in the text were produced by natural breeding according to the schemes presented in the Major Resources Tables (Table II in the online-only Data Supplement), and genotyping was performed using the primers also specified in the Major Resources Tables (Table III in the online-only Data Supplement). Embryos of both sexes were collected and used for the analyses as illustrated in Figure I in the online-only Data Supplement. However, no discrepancies between the genders were detected at E11.5, revealed by dividing the average RPKM expression levels of the Y chromosome expressed genes *Ddx3y*, *Eif2s3y*, and *Uty*, respectively, with the RPKM expression levels in the E11.5 RNA-Seq and E14.5 TRAP-Seq samples (Figure I in the online-only Data Supplement).

Animal care and research protocols were in accordance with institutional guidelines and approved by the appropriate Stockholm Norra Djurförsöks Etiska Nämnd or Cleveland Clinic committees. For staging of embryos, the morning of vaginal plug was designated as E0.5. To induce recombination in CreERT2 mice, tamoxifen (Sigma) was resuspended in corn oil (20 mg/mL) and administered by oral gavage (200 µL per mouse) at E8.5 to E10.5 as indicated.

Generation of R26-Axin1-IRES2-LacZ (R26Axin1IL, AOE) Mice

The R26-*Axin1*-IRES2-LacZ allele was generated by assembly of a construct containing the splice acceptor (SA) from pBigT, followed by the puromycin resistance gene, the bovine growth hormone polyA sequence, the CAGGS enhancer/promoter/intron/SA cassette from pCAGGS, a floxed tpA (3 SV40 polyA sequences from pBigT), a cassette containing IRES2-LacZ preceded by a nuclear localization signal and finally the pCAGGS polyA sequence. Subsequently, mouse *Axin1* gene was polymerase chain reaction amplified using the following primers: *Nhe*I-KOZAK-cmyc-m*Axin1*-5′ GGG AAA GCT AGC GCC GCC ACC ATG GAG CAA AAG CTC ATT TCT GAA GAG GAC TTG AAT GAA ATG AAT GTC CAG GAG CAG GG -3′ and *Sbf*I-5′ GGG AAA CCT GCA GGT CAG TCC ACC TTT TCC ACC T -3′ digested with *Nhe*I and *Sbf*I and subcloned in between the floxed tpA and IRES2LacZ cassettes into pBSApBpACAGftILn.[6] The conditional expression construct was released with *Pac*I and *Asc*I and subcloned into the *Pac*I and *Asc*I sites of pRosa26PAS.[37] The construct was linearized and electroporated into F1 ES cells.[38] Colonies were screened by polymerase chain reaction using the primers for Rosa26-WT sequence and Rosa26-SA sequence specified in Table III in the online-only Data Supplement. Positive colonies were expanded. One targeted clone was injected into host (C57BL/6J, Jackson Laboratories) blastocysts by the Karolinska Center for Transgene Technologies, Karolinska Institutet. Mice and embryos were genotyped using the primers against R26Axin1IL, or R26-wt as indicated in the Major Resources Tables (Table III in the online-only Data Supplement).

X-Gal Histochemistry

Slides were washed in PBS containing 0.02% NP-40 and 2 mmol/L MgCl2. The X-gal signal was detected with a solution consisting of 5 mmol/L K3Fe(CN)6, 5 mmol/L K4Fe(CN)6, 2 mmol/L MgCl2, 0.01% sodium deoxycholate, 0.02% NP-40, and 1 mg/mL X-gal at 37°C. The sections were counterstained with Nuclear Fast Red Solution (Sigma Aldrich, N3020).

Immunohistochemistry

Embryos were dissected and fixed in 4% paraformaldehyde for 2 hours followed by incubation in 15% sucrose for 4 hours and finally in 30% sucrose overnight, before embedding and snap freezing in OCT (optical coherence tomography freezing and embedding medium for cryosectioning; Leica, 14020108926). Cryosections (10–20 µm thick) were cut using a cryostat (Leica) and mounted on Superfrost Plus slides (Thermo Scientific, 4951PLUS4). Tissues were stained with the following primary antibodies (also listed in Table IV in the online-only Data Supplement) diluted in blocking solution (PBS, 3% BSA, and 0.25% TritonX-100) overnight at 4°C: Flk-1 (BD Biosciences, 555307) 1:1000, CD31/PECAM1 (R&D systems, AF3628) 1:1000, Glut1 (Santa Cruz Biotechnology, sc1605) 1:1000, Cldn5 (Life Technologies, 34–1600) 1:500. Cy3- or Alexa Fluor-coupled species-specific secondary antibodies (Molecular Probes, Jackson Immuno Research) were used at 1:1000. Antibody concentrations are listed in the Major Resources Tables (Table IV in the online-only Data Supplement). Mounting was done with ProLong Antifading reagent (Life Technologies, P36931) or Immu-Mount (Thermo Scientific, 99-904-02).

For chromogenic secondary detection, species-specific biotin-conjugated secondary antibodies (Jackson Immuno Research) were used together with the VECTASTAIN ABC system (VECTOR laboratories, PK-4000). Development was done with DAB (3′3 diaminobenzidine) peroxidase substrate solution (Sigma Aldrich, D8001) and before mounting with DPX (Sigma Aldrich, 06522) the slides were dehydrated in 70% ethanol for 1 minute, 95% ethanol for 1 minute, 99% ethanol for 1 minute, and xylene for 5 minutes. Negative controls were performed by the same conditions described above but by omitting the primary antibody or running with only IgG followed by Alexa Fluor-coupled secondary antibodies (Figure II in the online-only Data Supplement) as previously described.

Quantification of Pericyte Coverage

Pericyte abundance was evaluated by normalizing PDGFR-β (platelet-derived growth factor receptor beta) immuno-positive signals in a fixed area within the forebrain PVP to the size of the area leading to an estimation of the relative contribution of pericytes (in percent) to the tissue. Vessel-associated pericyte processes were evaluated as the percentage of the total pericyte signal that overlapped with the endothelial PECAM1 (platelet endothelial cell adhesion molecule; CD31 [cluster of differentiation 31]) immune-positive signal within a fixed area of the forebrain PVP.

Flatmount Immunofluorescence

E11.5 embryos were dissected from the yolk sac, genotyped, and fixed in 4% paraformaldehyde overnight, followed by overnight incubation in sterile 1×PBS. Telencephalic vesicles were dissected out from these embryos in sterile 1×PBS and incubated in block/permeabilization buffer (1% BSA, 0.5% TritonX-100 in PBS) overnight. The samples were incubated with the following primary antibodies (also listed in the Major Resources Tables [Table IV in the online-only Data Supplement]) for 48 hours; CD31/PECAM1 (R&D

systems, AF3628, goat IgG) 1:1000 and collagen IV (AbDSerotec, 2150-1470, rabbit IgG) 1:100 diluted in 1:1 mixture of block/permeabilisation buffer-PBS with or without 4% normal donkey serum. The tissue was washed with block/permeabilization buffer-PBS for 4×10 minutes and incubated with secondary antibodies (Alexa Fluor-coupled coupled secondary antibodies, Molecular Probes, 1:200) for 2 hours or +4C O/N and finally washed for 2×10 minutes in 1×PBS or with block/permeabilisation buffer-PBS for 4×10 minutes, rinsed in 1×PBS, and flatmounted on microscope slides (Superfrost Plus glass, Thermo Scientific, 4951PLUS4) with ProLong Antifading reagent (Life Technologies P36931). The flat mounts were achieved by 2 cuts through the neocortex exposing the intact medial ganglionic eminence (MGE) and lateral ganglionic eminence (Figure III in the online-only Data Supplement). Negative controls were performed by the same conditions described above but by omitting the primary antibody running with the only IgG followed by Alexa Fluor-coupled secondary antibodies (Figure II in the online-only Data Supplement) as previously described. Imaging was performed using a Zeiss confocal microscope (Zeiss LSM 510).

Flatmount Parametric Measurements and Statistical Analysis

Four areas within the MGE, (2 per telencephalic vesicle) per embryo were investigated. Photomicrographs of the MGE were taken from the perineural vascular plexus through radial vessels and PVP up to the stretching filopodia. Image analysis was performed with FIJI[39] using plug-ins for cell counting, branch identification and length, the number and diameter of radial vessels were calculated. A branch point was defined as a point where branching occurred in at least 3 directions. Diameters of PVP vessels were measured using ImageJ. In total, >1000 individual width measurements were averaged per embryo. Vascular regression was quantified as the number of red pixels in collagen IV (red) and PECAM1 (green) double-stained embryos (where collagen IV-positive vessels appear in yellow), converted to μm^2 and normalized to an area of interest of 1 mm^2, calculated using ImageJ. For each embryo, brain snapshots for each of the 2 brain hemispheres were quantified in a semiautomated manner and averaged. For all statistical comparisons, except Apod-stained tissues, 2-tailed heteroscedastic *t* tests with Welch correction were performed using Prism 6 (GraphPad Software). For Apod-stained tissues, the nonparametric Mann-Whitney test was used.

Leakage Studies

E12.5 mutant and control embryos underwent cardiac perfusion with Alexa Fluor 555-conjugated 70 kDa dextran (50 µL of 2.5 mg/mL in PBS; Invitrogen) using a pulled glass pipette with mouth connector and tubing (Sigma, P0799) in the course of the 15 to 20 minutes when a visible heart beat could be observed. Fluorescent visualization of the entire vasculature confirmed the perfusion. Tracer was left circulating for 10 minutes at room temperature, embryos were decapitated, their heads fixed in 4% paraformaldehyde overnight at 4°C, cryosectioned and stained as described above. Staining was performed with the following primary antibodies; CD31/PECAM1 (R&D systems, AF3628) 1:1000 and monoclonal TER-119 (R&D Systems, MAB1125) 1:250 followed by a 2 hours incubation at room temperature with DyLight Fluor-coupled secondary antibodies (1:1000, Thermo Scientific Pierce).

Sample Preparation for Flow Cytometric Quantification and Fluorescence Activated Cell Sorted

To obtain brain ECs, dams were sacrificed and ventral forebrains (MGE/lateral ganglionic eminence) were isolated. Genotyping was performed based on EGFP and *LacZ* expression. After isolation and dissection in ice-cold PBS (w/o Mg++ or Ca++, Gibco), an equal volume of a mixture of collagenase (2.5 mg/mL Worthington Biochemical Corporation LS004176) and DNase (30 U/µL, SIGMA, to a final of 0,04 mg/mL) in 37°C prewarmed PBS (Mg++ and Ca++, Gibco) was added for 15 to 30 minutes at 37°C on a shaker. Cells were filtered through a cell strainer (40 µm mesh, Falcon) followed by addition of 10% FBS:DMEM to a final volume of 6 mL and centrifugation at 800×*g*, +4°C for 5 minutes. The supernatant was removed, cells were incubated for 10 minutes in 500 µL blocking solution (2% FBS:PBS), divided in tubes as indicated in Table V in the online-only Data Supplement and stained with antibodies: CD31/PECAM1 PE (BD Biosciences, 553373) 1:1000, CD45 APC-CY7 (BD Biosciences, 557659) 1:100 or control $IgG_{2A,\ K}$ PE (affymetrix eBioscience, 12432181) and APC-CY7 (BD Biosciences, 552773) and incubated on ice for 10 minutes. Propidium iodide was included to distinguish between dead and living cells. Samples were washed with blocking solution (50 mL/condition) to remove any traces of remaining antibody followed by centrifugation (800×*g*, +4°C) for 5 minutes. Before flow cytometry cells were recovered in 1.5 mL of blocking solution.

Wnt Reporter Activity and Statistical Analysis

Axin1^{iEC-OE} mice were crossed into the Wnt-reporter mouse strain: Tg(TCF/Lef1-hIST1h2BB/EGFP)$^{61hadj/J}$.[35] *Axin1*$^{iEC-OE/GFP+}$ cells were analyzed as readout for Wnt signaling. Wnt-reporter activity using flow cytometric analysis (FACScalibur BD) was used (Table V in the online-only Data Supplement). For each sample, cell populations were discriminated from debris in the side scatter-forward scatter (FSC) dot plot. Singlet's gating was done in the FSC pulse area—FSC pulse width plot. Blood cells were gated out by CD45 labeling with CD45 APC-CY7 (BD Biosciences, rat IgG_{2B} 557659). The CD45 negative population was presented in the CD31/PECAM1 forward scatter dot plot for EC gating. Finally, the ECs were plotted in the PECAM1/GFP dot plot for determining the endothelial GFP positive/negative events. The percentage of GFP+CD45- versus total CD45- from 5 runs (n=5) were calculated and a 2-tailed heteroscedastic *t* tests with Welch correction were performed using Prism 6 (GraphPad Software) to gain statistical data of the Wnt positive ECs.

Sample Processing, RNA Sequencing, and Statistical Analysis

ECs from E11.5 ventral forebrains (MGE/lateral ganglionic eminence) were prepared, and ECs were labeled and flow sorted as described above. CD31/PECAM1 positive cells, obtained by fluorescence-activated cell sorting (FACS) using MoFlo XPD (Beckman Coulter), were further processed for total RNA (RNeasy Micro Kit no. 74004, Qiagen) followed by pre-RNA Sequencing procedures. ECs from E14.5 forebrains were prepared as described in Hupe et al.[30] In brief, libraries were prepared using SMARTer Ultra Low Input RNA for Illumina. Sequencing kit (Clontech) and sequenced on an Illumina HiSeq 2000. Reads were aligned using Bowtie 0.12.7[40] to the genome (assembly mm^9) and transcriptome (Ensembl annotation, downloaded May 16, 2011). Transcriptome-mapped reads were translated to genome coordinates, merged with genomic alignments, and nonuniquely aligning reads were discarded. We then calculated expression values and read counts using rpkmforgenes (available at http://sandberg.cmb.ki.se/rnaseq/)[41] with settings—full transcript—mRNAnorm and RefSeq gene annotation from July 31, 2011. RPKM values for constructs were calculated from counting bowtie alignments and normalized by lengths and the normalization read sum from rpkmforgenes. Raw data and expression values have been deposited to NCBI Sequence Read Archive with ID SRP056125 and Gene Expression Omnibus with ID GSE66848. For differential expression testing, we used a similar test as previously described.[29] False discovery rates were calculated by the Benjamini-Hochberg method. Genes with <5% false discovery rate were considered differentially expressed. For the E14.5 *Axin1*$^{iEC-OE}$ (Gene Expression Omnibus entry: GSE66848) and *Ctnnb1KO*^{iEC} samples,[30] we applied a <5% false discovery rate cutoff to the DESeq *P* values. These samples had been prepared according to endothelial-specific TRAP sequencing.[31]

Zebrafish Lines and Care

Zebrafish and embryos were maintained, handled, and raised under standard conditions as previously described.[25] Transgenic and mutant lines used include *Tg(Kdrl:*EGFP)^{s843}, *Tg(Kdrl:*hsa.HRAS-mCherry)^{s896}, *Tg(Hsp70l:*Mmu.Axin1-YFP)^{w35}, and *Adgra2*^{s984}.[25,42–44]

Zebrafish Manipulations, Imaging, and Statistical Analysis

Capped-RNA was synthesized from full-length mouse *Adamtsl2* template (IMAGE ID 40097418, LifeSciences) using the mMessage mMachine SP6 kit (Ambion, Carlsbad, CA) and injected at the 1-cell stage at 100 pg. Heat-shock was performed on manually dechorionated embryos at 26 or 30 hpf replacing the medium with prewarmed 38°C egg-water and subsequent incubation for 50 minutes. Sixty hours postfertilization embryos and 72 hpf larvae were anesthetized and mounted in 1% Ultrapure LMP Agarose (Invitrogen, Waltham, MA) in glass-bottom dishes (MatTek Corporation, Ashland, MA). Images were acquired using a Zeiss LSM710 confocal microscope (Oberkochen, Germany). Hindbrain cerebral central arteries (CtAs) were quantified and assessed for lumenization. Basilar artery connections were quantified as the total number of CtAs connecting from both hemispheres to the basilar artery. Nonparametric Mann-Whitney test was used to analyze the data by Prism 6 (GraphPad Software).

Results

Vascular Endothelium-Specific Axin1 Overexpression Leads to Moderately Repressed β-Catenin Signaling in the Forebrain

To study the role of Axin1-mediated repression of β-catenin signaling in ECs during different stages of CNS vascular development, we generated R26-Axin1-IRES2lacZ mice that allowed us to conditionally overexpress Axin1 (AOE) on induction of Cre-mediated recombination (Figure 1A). Our targeting design also allowed visualization of recombination events using β-galactosidase staining. Importantly, crossing these mice to the EC-specific and inducible *Cdh5:*CreERT2 mouse line allowed induction of AOE in vascular ECs (*Axin1*$^{iEC-OE}$) by administration of tamoxifen at developmental stages of interest (Figure 1A).[32,33] Tamoxifen treatment at E9.5

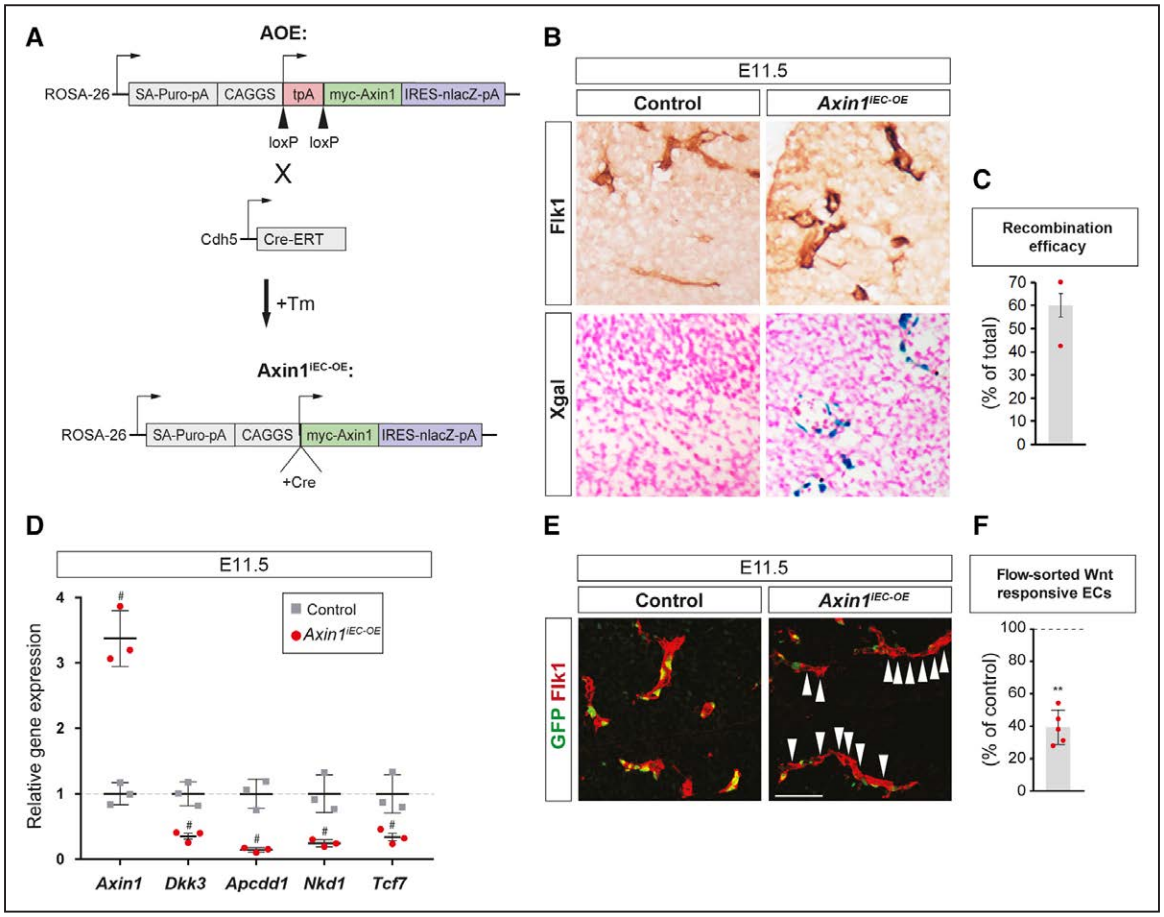

Figure 1. Overexpression of Axin 1 (AOE) specifically in endothelial cells (ECs) results in inhibition of Wnt/β-catenin pathway activity in mice. **A**, Schematic representation of the targeting cassette containing a myc-tagged Axin1-IRES-lacZ construct used to generate the conditional AOE mouse strain. By crossing to Cdh5: CreERT2 or Flk1:Cre mice Axin1 was overexpressed specifically in ECs. **B**, Immunostainings for the EC-specific marker Flk-1, (**top** row) and β-galactosidase activity assays performed on adjacent sections, revealing Cre-mediated transgene activation (**bottom** row, **right**), in the vessels. **C**, Quantification of the number of Flk-1 positive ECs showing β-galactosidase activity 48 h after tamoxifen injection at E11.5. n=16 regions of interest from 5 slides and 2 mice. $P<0.002$. **D**, Axin1 mRNA was moderately overexpressed by 3.2-fold in ECs on Cre-mediated recombination compared with wildtype embryos whereas Wnt downstream target genes were significantly downregulated, as assessed by RNA-Seq analysis ($P<0.001$, SAM [significance analysis of microarrays] test, n=3, # denotes false discovery rate<0.05). **E**, Confocal imaging of coronal forebrain sections of *Axin1*$^{iEC-OE}$ mouse embryos that express EGFP (GFP) on Wnt-signaling activation reveals that already 2 d after EC-specific Cre-induction, GFP (green) is lost in most ECs (white arrowheads) as identified by immunostaining for Flk-1 (red). Scale bar =50 μm. **F**, Quantification of EGFP (GFP)-signal intensity in ECs normalized to controls by flow cytometry analysis indicates that Wnt-signaling is significantly downregulated in ECs of *Axin1*$^{iEC-OE}$ mouse embryos (n=5, $P<0.01$). For each flow cytometry experiment 2–4 embryos were pooled. n=5 experiments. Students *t* test was performed. $^{**}P<0.01$. All error bars indicate ±SD. SA indicates splice acceptor site; and tpA, 3 SV40 polyA sequences from pBigT.

in *Axin1*$^{iEC-OE}$ heterozygous carriers led to Cre-mediated recombination and robust expression of LacZ in ≈60% of the forebrain ECs at E11.5 (Figure 1B and 1C). RNA Smart-Seq analysis on FACS ECs revealed that Axin1 expression was elevated by 3.2-fold in the entire EC population under these conditions, implying a ≈5-fold induction of Axin1 in recombined ECs (Figure 1D). Consistent with the role of Axin1 in inhibition of canonical Wnt-signaling, we found a robust downregulation of Wnt-target genes, including *Dkk3*, *Apcdd1*, *Nkd1*, and *Tcf7* in the *Axin1*$^{iEC-OE}$ mutants (Figure 1D).

To further validate reduced Wnt-signaling activity in our *Axin1*$^{iEC-OE}$ mutants in vivo, we crossed *Axin1*$^{iEC-OE}$ mice into an established Wnt-reporter mouse model expressing EGFP (enhanced green fluorescent protein) under the *Tcf/Lef1* promoter in ECs. We detected a strong reduction in the EGFP signal in Flk1 (fetal liver kinase 1, also known as Kdr:kinase insert domain receptor, encoding Vegf-r2 [vascular endothelial growth factor receptor 2]) positive ECs compared with control reporters (Figure 1E). Furthermore, we labeled ECs with an anti-PECAM1 (CD31) antibody in our Wnt-reporter mice and

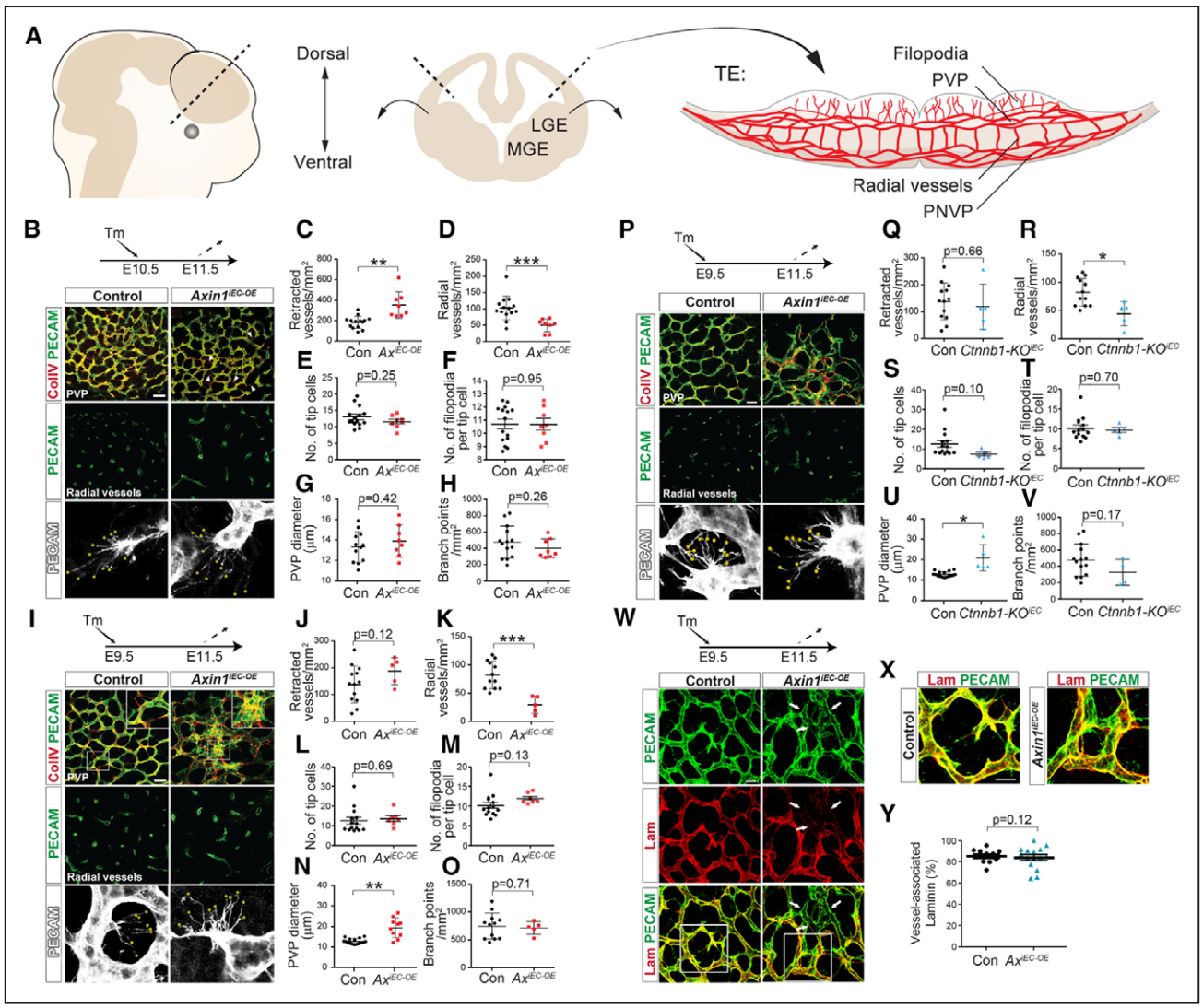

Figure 2. Vascular regression followed by dilation without pericyte loss in the forebrain upon endothelial cell (EC)-specific Axin1 overexpression (AOE). **A**, Schematic illustration of the flat mounting protocol for visualization of the embryonic telencephalon (TE) and its vascular layers. The dorsal telencephalon is surgically removed and the ventral underlying layers are flattened out enabling accurate imaging of the vasculature (See also Figure III in the online-only Data Supplement). Confocal imaging of immunostained flat-mounted forebrains from *Axin1*$^{iEC-OE}$ (**B–Y**) Cdh5CreERT2;R26Axin1IL^{het} (**B–O** and **W–Y**) and *Ctnnb1*-KO^{IEC} (**P–V**) embryos at E11.5, 1 d (**B–H**) or 48 h (**I–Y**) after Cre-induction. Basement membrane markers collagen alpha-4(IV) chain (ColIV) (**B–V**), or Laminin subunit α4 (Lam) (**W–Y**) are shown in red and ECs are stained with an anti-PECAM1 antibody in green. The first row of each panel in **B**, **I**, and **P** show perivascular plexus (PVP), second row shows the underlying radial vessels and filopodia from tip cells are displayed in the third row (marked by white, anti-PECAM1 stain). Vessel morphology was characterized by retracted vessel density (**C**, **J**, **Q**, and **S2**), radial vessel density (**D**, **K**, **R**, and **S2**), number of tip cells (**E**, **L**, **S**, and **S2**), number of filopodia/tip cell (**F**, **M**, **T**, and **S2**) and PVP vessel diameter (**G**, **N**, **U**, and **S2**), branch points (**H**, **O**, **V**, and **S2**). Twenty-four hours after Cre-induction, significant differences in the density of retracted and radial vessels are detected in *Axin1*$^{iEC-OE}$ embryos (**C** and **D**). Forty-eight hours after Cre-induction, the density of radial vessels is still significantly reduced in *Axin1*$^{iEC-OE}$ (**K**) and *Ctnnb1-KO*^{IEC} mutant embryos (**R**). Furthermore, PVP vessels are significantly dilated (**N** and **U**). Quantifications of vessel-associated laminin-α4 (**Y**), indicate that this parameter is not significantly changed in *Axin1*$^{iEC-OE}$ embryos. Note that the vascular phenotypes of *Axin1*$^{iEC-OE}$ and *Axin1*$^{iEC-OE}$ mutant embryos are overall very similar. White boxes in **W** indicate the areas magnified in **Y**. White arrows in **W** indicate an area of reduced Laminin coverage. LGE indicates lateral ganglionic eminence; MGE, medial ganglionic eminence; NS, nonsignificant; and PNVP, perineural vascular plexus. **P*<0.05; ***P*<0.01; ****P*<0.001; all error bars indicate ±SD. All scale bars =50 µm.

performed flow cytometry counting to quantify the reduction in EGFP-expression (Figure 1F). Both methods independently confirmed that Wnt-signaling was downregulated in ECs in *Axin1*$^{iEC-OE}$ mutant mice to ≈40% of that seen in controls.

Inhibition of Canonical Wnt-Signaling Results in Immediate Forebrain Vascular Regression and Remodeling

EC-specific deletion of β-catenin is known to culminate in severe vascular malformation and hemorrhage in the entire CNS.[6] To examine the underlying causes of these severe vascular phenotypes and understand the role of Axin1 in this context, we analyzed forebrain vascular phenotypes 24 and 48 hours after tamoxifen-induced recombination in *Axin1*$^{iEC-OE}$ mice. To accurately visualize the 3-dimensional vascular architecture of the embryonic telencephalon, that is, the forebrain area where reduced β-catenin signaling was observed in *Axin1*$^{iEC-OE}$ mice, we first developed a protocol for generating open book flat-mount preparations of this tissue (Figure 2A; Figure III in the online-only Data Supplement). Cre-expression was induced in *Axin1*$^{iEC-OE}$ mice at E9.5 or E10.5 and animals were euthanized for flat-mount preparations at E11.5, (Figure 2B through 2Y). Already after 24 hours of *Axin1*$^{iEC-OE}$, we found significant retraction of capillaries in the PVP, as judged by the appearance of empty, collagen IV positive basement membrane sleeves of *Axin1*$^{iEC-OE}$ mice (Figure 2B and 2C). While the number of tip cells, filopodia, and PVP branch points were unaffected (Figure 2B, 2E, 2F, and 2H), the number of radial vessels (Figure 2D) were significantly reduced, indicating impaired vascular stability but not sprouting shortly after reducing β-catenin signaling. After 48 hours of *Axin1*$^{iEC-OE}$, while there was no longer any increase in PVP vessel retraction (Figure 2I and 2J), the number of radial vessels were still reduced compared with control mice (Figure 2I and 2K). Also at 48 hours of *Axin1*$^{iEC-OE}$, the number of tip cells, filopodia, and branch points did not change (Figure 2I, 2L, 2M, and 2O). However, a significant increase in vessel diameter in the PVP was observed, which had not yet developed at 24 hours of *Axin1*$^{iEC-OE}$ (Figure 2B, 2G, 2I, and 2N). Importantly, EC-specific loss-of-function mutants of β-catenin (*Ctnnb1-KO*^{iEC}), at E9.5 phenocopied the vascular changes in the forebrain of *Axin1*$^{iEC-OE}$ at E11.5 (Figure 2P through 2V) thus substantiating that the effects we observed in the latter were caused by overall reduced Wnt-signaling activity.

Vascular remodeling in the CNS is often accompanied or caused by impaired basement membrane formation and coverage with vascular mural cells.[1] To examine, if this was also the case in *Axin1*$^{iEC-OE}$ mice, we stained the basement membrane with anti-Laminin-α4 antibodies and the mural cells with anti-Pdgfrβ antibodies (Figures 2W through 2Y and 3A through 3D). Forebrain vessels in both control and *Axin1*$^{iEC-OE}$ mice exhibited robust coverage overall by Laminin-α4 at E11.5 (Figure 2W through 2Y). *Axin1*$^{iEC-OE}$ mice did, however, exhibit areas with reduced basement membrane coverage (Figure 2W), suggesting that vascular maturation might be delayed in the PVP of *Axin1*$^{iEC-OE}$ compared with control mice. Similarly, vascular coverage by Pdgfrβ-positive mural cells was as expected rather poor but similar in both control and *Axin1*$^{iEC-OE}$ mice overall (Figure 3A through 3D). The same areas exhibiting reduced basement membrane coverage (Figure 2W and 2X), however, also demonstrated a lack of mural cell cells (Figure 3B), suggesting that mural cell recruitment and basement membrane formation may coincide during development and is delayed focally in *Axin1*$^{iEC-OE}$ mice.

Axin1^{iEC-OE} Leads to Impaired CNS Vascular Maturation and Stability in Zebrafish

To study the temporal role of β-catenin in CNS angiogenesis and vascular maturation in more detail, we analyzed EC invasion, angiogenesis, vascular stability, and maturation in the

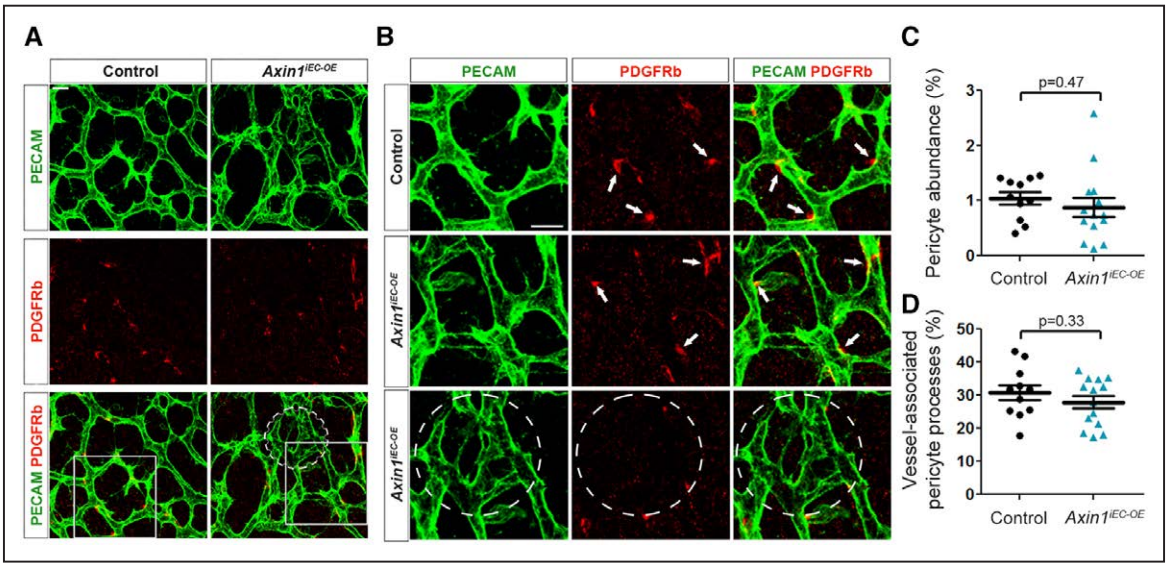

Figure 3. Pericyte coverage of the forebrain perivascular plexus (PVP) is not globally impaired in *Axin*$^{iEC-OE}$ mice. Confocal imaging of immunostained flat-mounted forebrains from *Axin1*$^{iEC-OE}$ and control embryos at E11.5, 48 h after Cre-induction. Pdgfr-β expression by pericytes is shown in red (PDGFRb) and endothelial cells (ECs) are stained with an anti-PECAM1 (CD31) antibody shown in green (**A** and **B**). Relative percentage of the tissue consisting of pericytes (**C**) and percentage of the pericyte signal associated with the endothelium (**D**) was quantified. White boxes in **A** indicate the regions magnified in **B**. White arrows in **B** indicate pericytes. White dashed circle in **A** and **B** indicate an area of reduced pericyte coverage.

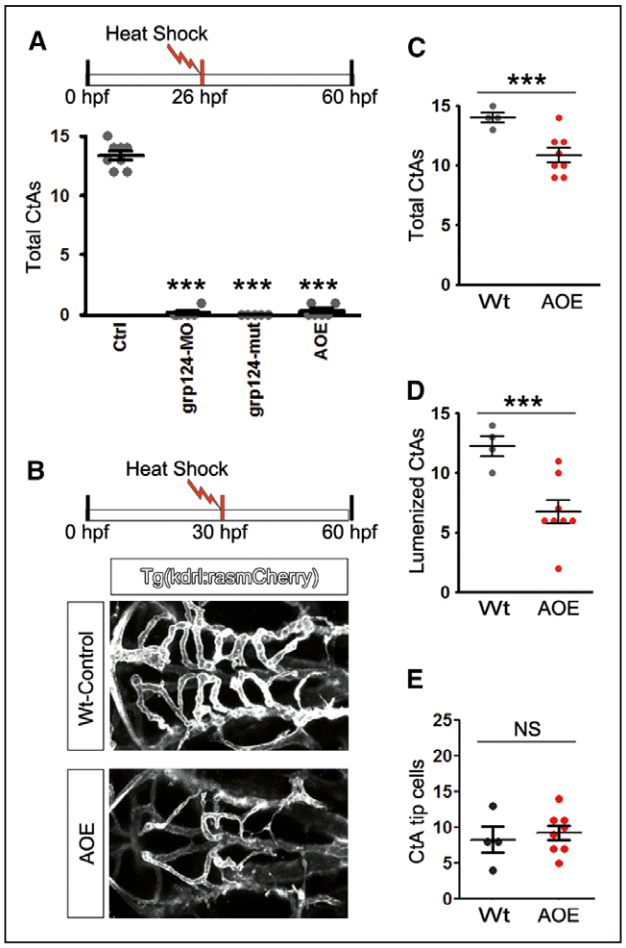

Figure 4. Brain vascular maturation and stability are compromised in zebrafish upon *Axin1*$^{iEC-OE}$. **A**, **Top**: Experimental design. **Bottom**: Quantification of the number of central arteries (CtAs) formed at 60 h postfertilization (hpf) in *Tg(kdrl*:rasmCherry; Wt, Ctrl), *Tg(adgra2*^{s984}*;kdrl*:rasmCherry; gpr124-mut), grp124-morpholino-injected *Tg(kdrl*:rasmCherry; grp124-MO) at the 1-cell stage or *Tg(hsp70l*:Mmu.Axin1-YFP;*kdrl*:rasmCherry) zebrafish embryos following heat-shock induced Axin1 overexpression at 26 hpf (AOE). ***P<0.001. **B**, Confocal micrographs of the central arteries in Wt or AOE zebrafish embryos at 60 hpf, exposed to heat-shock–induced AOE at 30 hpf. **C–E**, Quantification of the total number of CtAs (**C**), lumenized CtAs (**D**), or CtA tip cells (**E**) from the experiment shown in **B**. n=4–8 as indicated. NS indicates nonsignificant. ***P<0.001.

CNS of inducible β-catenin loss-of-function zebrafish models. Consistent with previous findings,[25] *gpr124* mutants or morphants that are unable to induce β-catenin signaling in ECs or embryos conditionally AOE on heat shock at 26 hpf, that is, just before initial EC invasion into the CNS (corresponding to E8.5 in mice), were unable to form a CNS vasculature and completely lacked CtAs at 60 hpf (Figure 4A). Heat-shocking embryos at 30 hpf, a few hours after the initial vascular invasion of the CNS (corresponding to E9.5 in mice), however, did not completely impair CNS vascular development but AOE still resulted in a dramatic reduction of total and lumenized CtAs at 60 hpf, while not affecting the formation of endothelial tip cells in the brain (Figure 4B through 4E). This suggested that β-catenin signaling is important for CNS vascular stability but not ongoing angiogenesis from 30 hpf onwards (ie, after initial invasion), similar to our findings in *Axin1*$^{iEC-OE}$ mice.

Long-Term *Axin1*$^{iEC-OE}$ Causes Forebrain-Specific Hemorrhage

To analyze long-term effects of AOE during mouse development, we investigated if and when CNS hemorrhaging occurred in EC-specific constitutively AOE, *AOE*^{Flk1} mice. These mice developed without pronounced vascular phenotypes until E11.5, but at E12.5 robust hemorrhage could be observed specifically localized to the forebrain (Figure 5A). To analyze whether Wnt-signaling was important in a particular window during development, we induced AOE at E8.5, E9.5, or E10.5 in *Axin1*$^{iEC-OE}$ mice and analyzed brain hemorrhage phenotypes from E12.5 onwards. Induction of *Axin1*$^{iEC-OE}$ at E8.5 phenocopied the forebrain hemorrhage observed using constitutive *Axin1*^{Flk1} mice at E12.5 consistent with ECs invading the CNS and requiring β-catenin signaling from E8.5 onwards (Figure 5A). Postponing the induction of Axin1 to E9.5 resulted in a delay in forebrain hemorrhage which was not evident at E12.5 but instead prominent at E13.5 (Figure 5B). *Axin1*$^{iEC-OE}$ in these mice did not result in premature death, as a Mendelian 50% of the recovered embryos were *Axin1*$^{iEC-OE}$ mutants and 50% Cre-negative controls (Figure 5D). The penetrance of forebrain hemorrhage within the *Axin1*$^{iEC-OE}$ population was ≈25% (±6%), and as expected 0% (±0%) in the Cre-negative control population (Figure 5E). As the BBB is thought to be developed at E13.5,[45] we hypothesized that β-catenin signaling would be particularly important at the developmental window immediately before and including E13.5. Surprisingly, however, induction of AOE at E10.5 delayed both the onset and penetrance of forebrain hemorrhage until E14.5 (Figure 5C), whereas no hemorrhage could be observed at E13.5 in these mice. This suggested that 4 days of *Axin1*$^{iEC-OE}$ are required to develop forebrain hemorrhage regardless of the developmental window (ie, E8.5–E12.5, E9.5–E13.5, or E10.5–E14.5) during which AOE was induced. These findings are supported by previous observations from our and other laboratories that brain hemorrhaging was observed in many different Wnt-pathway mutants, including *Wnt7a*, *Wnt7b*, *Fz4*, *Lrp5*, *Lrp6*, and *Ctnnb1* single or compound deficient strains,[6,9] suggesting that the observed effects on impaired CNS vascular integrity are not Axin1-specific but rather are because of overall perturbed Wnt-signaling activity in ECs. In these other models of perturbed Wnt/β-catenin signaling, bleeding is, however, also observed in other brain regions as well as the spinal cord, whereas in the *Axin1*$^{iEC-OE}$ embryos, the phenotype was restricted to the ventral forebrain. This suggests that while β-catenin is important for maintaining the structural integrity of all CNS vessels, Axin1 is mainly involved in vascular destabilization because of reduced β-catenin signaling in the forebrain ECs.

Cerebral hemorrhage in adults often results from underlying cardiovascular problems such as hypertension. To investigate if *Axin1*$^{iEC-OE}$ embryos (E13.5) exhibited anatomic indicators of changes in cardiac output, which potentially could lead to general or local forebrain hypertension, we dissected the hearts of *Axin1*$^{iEC-OE}$ and control littermates and compared their forebrain vascular anatomy. The hearts of *Axin1*$^{iEC-OE}$ embryos were morphologically indistinguishable from controls without cardiac indicators of hypertension such as left ventricular hypertrophy or dilation (Figure 5F). Furthermore,

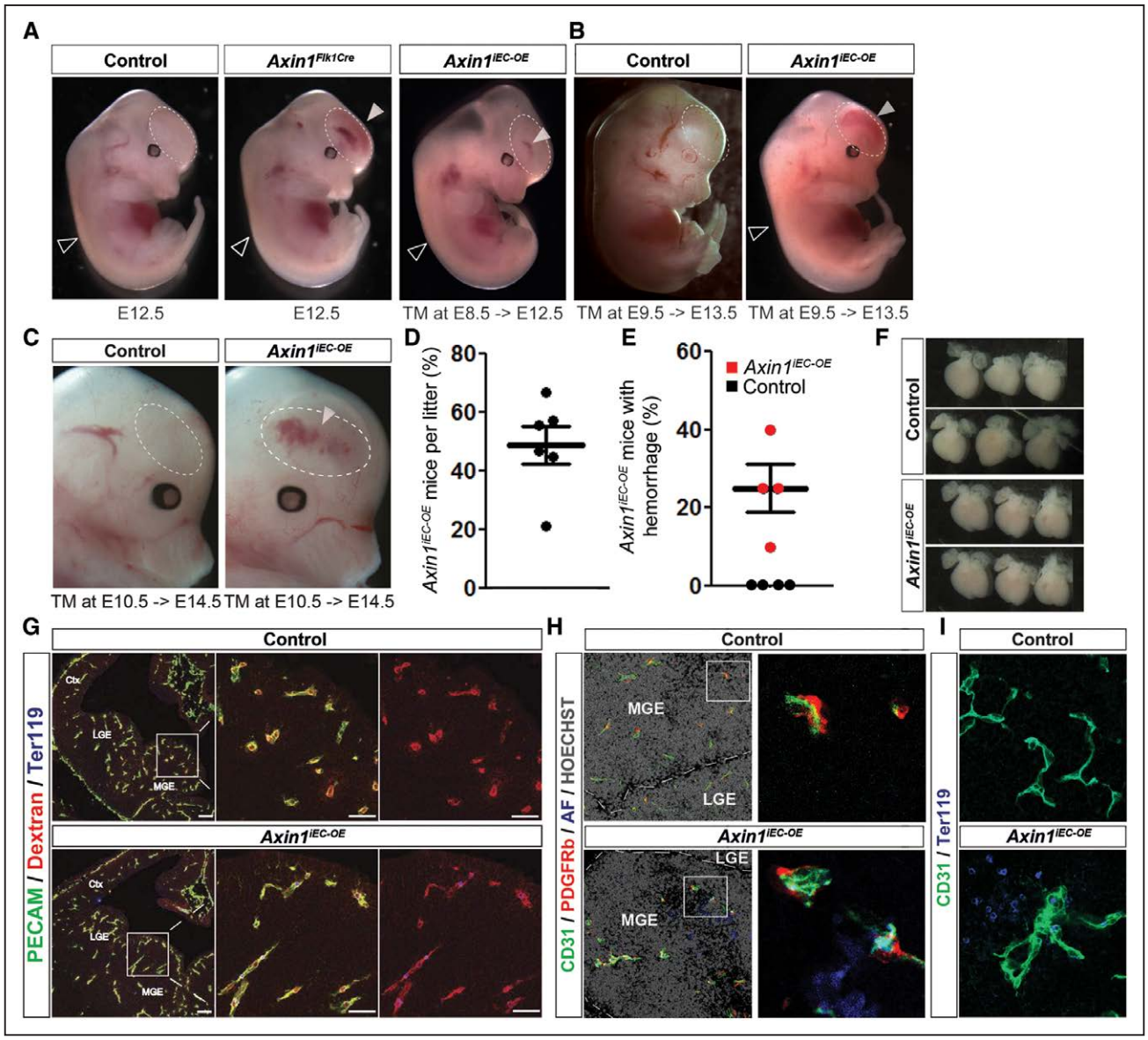

Figure 5. Axin1 overexpression (AOE) in endothelial cells (ECs) induces forebrain hemorrhage without prior vascular leakage or pericyte detachment during embryonic development. **A**, Stereomicroscopic images of E12-12.5 control and AOE^{Flk1} (Flk1:Cre;R26Axin1IL^{het}) showing hemorrhaging similar to *Axin1*$^{iEC-OE}$ embryos. White arrow indicates forebrain hemorrhage, black arrow indicates absence of hemorrhage in the spinal cord. **B**, *Axin1*$^{iEC-OE}$ mouse embryos display forebrain hemorrhaging at E13.5, 4 d post tamoxifen administration. **C**, *Axin1*$^{iEC-OE}$ mouse embryos display forebrain hemorrhaging at E14.5, 4 d post tamoxifen administration. **D**, Quantification of the number of Cre+ (ie, *Axin1*$^{iEC-OE}$) relative to Cre– embryos at E13.5, 4 d post tamoxifen administration. **E**, Quantification of the percentage of control (black) and *Axin1*$^{iEC-OE}$ (red) embryos at E13.5, 4 d post tamoxifen administration, presenting with forebrain hemorrhage. **F**, Stereomicroscopic images of E13.5 control and *Axin1*$^{iEC-OE}$ mouse hearts showing no differences in gross anatomy of the heart between the groups. **G**–**I**, Confocal images of frozen sections from E13.5 control or *Axin1*$^{iEC-OE}$ embryo forebrains (MGE [medial ganglionic eminence] and LGE [lateral ganglionic eminence] are indicated in **G**) stained with antibodies recognizing CD31-expressing ECs (green), TER119-expressing or autofluorescent (AF) erythroblasts and erythrocytes (blue), or Pdgfr-β-expressing pericytes (red in **H**), or injected with Alexa-555-labeled 70 kDa dextran (red in **G**). Counterstaining with Hoechst in **H** is shown in gray. Boxed regions are shown in the magnified images to the right. Size bars indicate 50 μm. sc indicates spinal cord; tel, telencephalon.

the forebrain vasculature was well perfused, and the vessels were of similar or larger caliber in *Axin1*$^{iEC-OE}$ mice compared with controls (Figure 5G) suggesting that the local blood pressure in the forebrain was likely not increased in *Axin1*$^{iEC-OE}$.

To investigate if the BBB breaks down before hemorrhaging, we next determined the severity/extent of leakage in the embryonic brain at E12.5, that is, 3 days after *Axin1*$^{iEC-OE}$ and one day before hemorrhage. Because the BBB gradually forms and tightens, in a size-selective manner over time, small molecular weight substances (≤10 kDa) leak spontaneously in embryonic forebrains at stages before E14.5[45] under physiological conditions. However, tracers with a higher molecular weight (ie, ≥70 kDa) are restricted within the forebrain vasculature already from E11.5 onwards.[46] Therefore, we applied 70 kDa dextran by cardiac perfusion and followed the perfusion and leakage of this tracer at E12.5. Leakage of 70 kDa dextran or extravasation of TER119+ erythroblasts or mature erythrocytes were not observed in *Axin1*$^{iEC-OE}$ mice compared with controls (Figure 5G), indicating that vascular integrity was not severely compromised 3 days after AOE. Furthermore, pericyte recruitment or pericyte-EC

interaction, an important feature of the developing and maturing BBB,[47,48] was not impaired in *Axin1*$^{iEC-OE}$ mice, as demonstrated by comparable PDGFRβ-positive mural cell numbers and vascular coverage even in hemorrhaging areas of the forebrain vasculature at E13.5 (Figure 5H and 5I). Collectively, these findings indicate that AOE in our *Axin1*$^{iEC-OE}$ mouse line induces inhibition of Wnt-signaling in ECs, which leads to progressive vascular destabilization, regression, and dilation.

Identification of Wnt/β-Catenin Regulated Genes in Forebrain ECs

To investigate the mechanisms of Wnt-β-catenin signaling specifically in forebrain ECs during CNS vascular development we isolated mRNA from forebrain ECs of 3 independent β-catenin loss-of-function mouse models: (1) *Axin1*$^{iEC-OE}$ embryos at E11.5 (ie, before BBB formation), (2) *Axin1*$^{iEC-OE}$ embryos at E14.5 (ie, after BBB formation) by TRAP (translating ribosome affinity purification),[30,31] and (3) *Ctnnb1*-KO^{iEC} embryos at E14.5 (here data were acquired from our previously published resource[30]), in all cases 48 hours after induction of Cre-mediated recombination. RNA was used for RNA Smart-Seq[29] (Figure 6A). Importantly, our cell preparation was pure and viable as cells were negative for propidium iodide and no significant neural, glial, and pericyte contaminations were detected in the RNA Smart-seq data set (Table VI in the online-only Data Supplement). After correcting for multiple testing, we found 455 genes significantly upregulated and 128 genes downregulated in *Axin1*$^{iEC-OE}$ mice at E11.5 on a genome-wide scale (Figure 6B). EC-specific receptors, such as Kdr (Flk1), Flt1 (FMS-like tyrosine kinase 1, encoding vascular endothelial growth factor receptor 1), Gpr124, and Reck, were not differentially expressed at E11.5 and only Reck was slightly downregulated in *Axin1*$^{iEC-OE}$ embryos at E14.5 (Figure 6C), suggesting that canonical Wnt-signaling is not involved in maintaining endothelial identity per se during CNS vascular development but could as previously reported[6] be involved in specifying CNS-specific endothelial characteristics. To test this hypothesis, we investigated the expression of EC-specific Wnt-pathway receptors at E11.5 and E14.5. Genes encoding Wnt-receptors Gpr124, Reck, FZD4, FZD6, FZD10, Lrp5, and Lrp6 were not differentially regulated at E11.5 but became either upregulated (FZD4) or downregulated (FZD6, FZD10, Lrp6, and Reck) at E14.5 in either *Axin1*$^{iEC-OE}$ (Lrp6 and Reck) or both *Axin1*$^{iEC-OE}$ and *Ctnnb1-KO*^{iEC} mice (FZD6 and FZD10; Figure 6C). The endothelial Wnt-target Tnfrsf19/Troy was downregulated under all 3 conditions (Figure 6C). Other BBB markers, such as Slc2a1 (Glut1 [solute carrier family 2, facilitated glucose transporter member 1]), Abcb1a, Slc7a5, Slco1c1, Slco2b1, and Ocln,[49] were downregulated at both developmental time points and in both mouse strains, and Slc7a1 became downregulated at E14.5, whereas Jam2 was only downregulated at E11.5 (Figure 6D and 6E), consistent with previous studies.[6] In contrast, the bonafide tight junction marker Cldn5, which is expressed by all tight junction-bearing ECs,[50] was upregulated at E11.5, but downregulated at E14.5, suggesting a differential role for β-catenin signaling in regulating tight junction formation at early and later stages of brain vascular development (Figure 6E). To further study whether Cldn5 and the BBB-marker Glut1 were also regulated at the protein level we performed immunohistochemistry of E11.5 *Axin1*$^{iEC-OE}$ and control mice 48 hours after tamoxifen injection (Figure IV in the online-only Data Supplement). In agreement with our RNA-seq data, Glut1 staining was reduced, although with borderline significance (P=0.054) in the *Axin1*$^{iEC-OE}$ mice, but Claudin-5 staining was significantly reduced in *Axin1*$^{iEC-OE}$ mice, suggesting that the

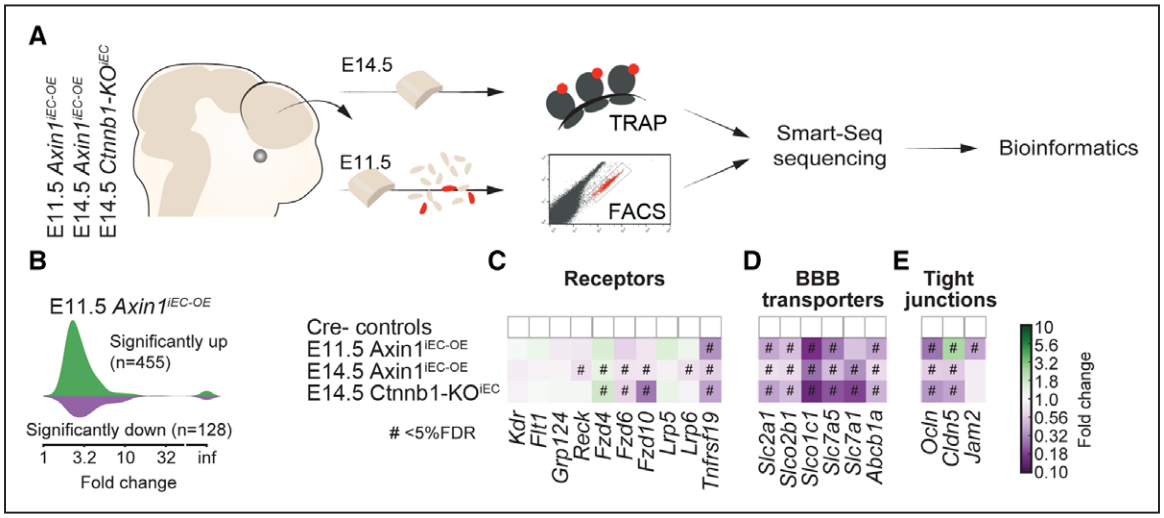

Figure 6. RNA expression profiling of the developing β-catenin–signaling deficient forebrain reveals impaired acquisition of central nervous system (CNS)-specific endothelial cell (EC)-phenotypes. **A**, Schematic representation of workflow. FACS profiling of *Axin1*$^{iEC-OE}$ forebrain-derived cells: scatter plot of PECAM1 (CD31+) reactivity vs propidium iodide (PI) reactivity of mouse forebrain cells at E11.5. The boxed region indicates the viable EC fraction used for RNA sequencing (Table VI in the online-only Data Supplement). Translating ribosome affinity purification (TRAP)-Seq was performed on Cdh5CreERT2$^{+/-}$;mCherryTRAP$^{+/-}$ AxinIL$^{+/-}$ forebrain at E14.5 and resource data from Cdh5CreERT2$^{+/-}$;mCherryTRAP$^{+/-}$ Ctnnb1$^{flox/flox}$ forebrains were used. **B**, Number of genes differently expressed in control and mutant forebrain ECs at E11.5 using identical bioinformatics conditions as **C–E**, at 5% false discovery rate (FDR). **C–E**, mRNA-Seq data for selected genes from forebrain ECs of control (**top** rows), *Axin1*$^{iEC-OE}$ (Cdh5ERT2;Cre;R26Axin1IL^{het}) mouse embryos at E11.5 (second rows) or E14.5 (Cdh5CreERT2$^{+/-}$;mCherryTRAP$^{+/-}$ AxinIL^{het}, third rows) or of Ctnnb1-KO^{IEC} (+/–;mCherryTRAP$^{+/-}$ Ctnnb1$^{flox/flox}$, lower rows) mouse embryos at E14.5, in all cases normalized to the levels of control embryos and done 48 h after Cre-induction. Genes with <5%FDR are marked with # (SAM [significance analysis of microarrays] test, n=3). The color represents the relative expression level as demonstrated in the bar to the right (**E**).

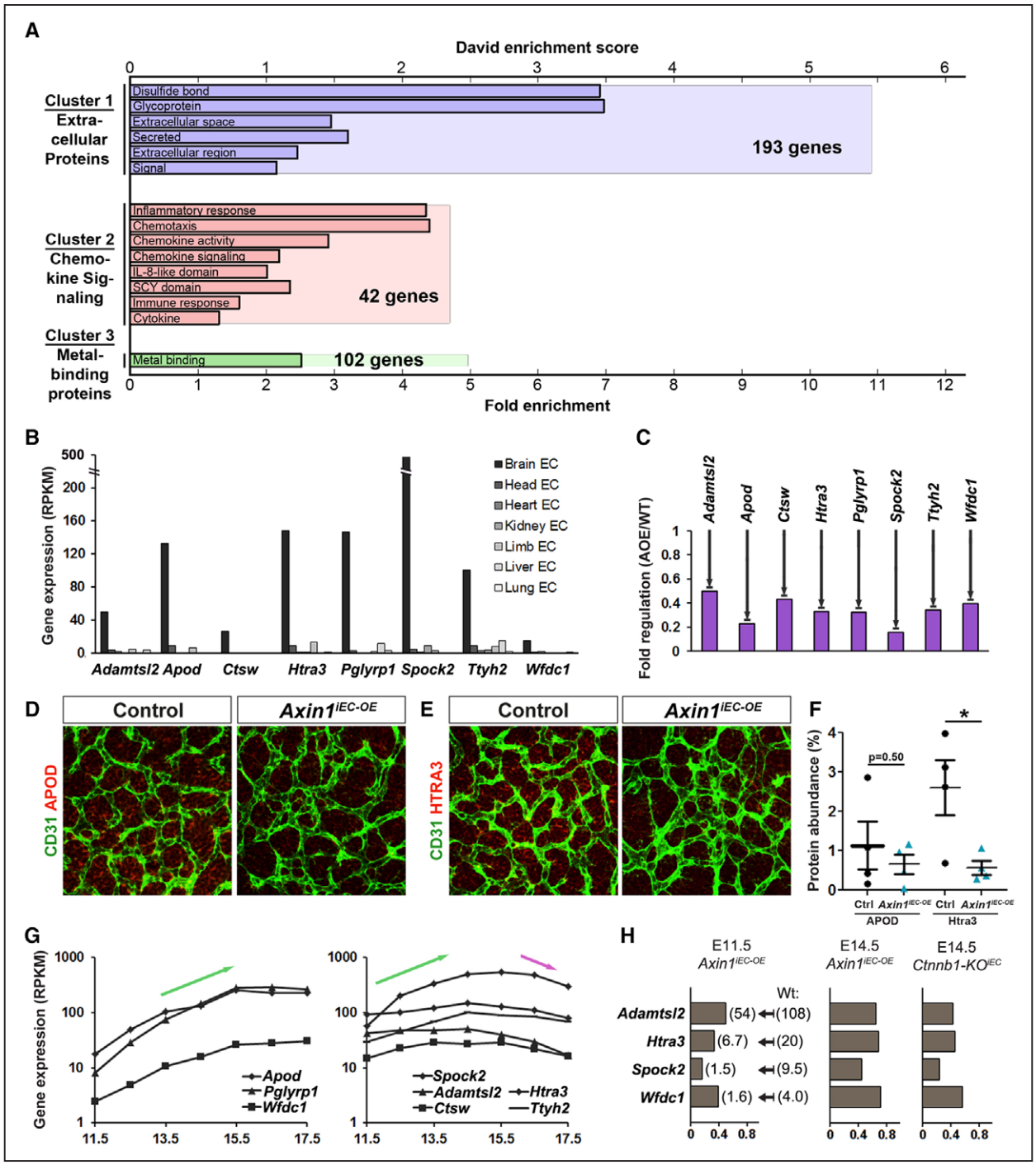

Figure 7. A forebrain vessel specific ECM (extracellular matrix) signature contribute to central nervous system (CNS) vascular maturation. **A**, DAVID pathway analysis of functional clusters of deregulated genes in endothelial cells (ECs) isolated as in 5A through 5E from E11.5 *Axin1*$^{iEC-OE}$ mouse embryos, 2 d after Cre-induction. Three clusters were significantly enriched (false discovery rate [FDR]<0.1) with the number of genes in each cluster indicated, full cluster bar and the corresponding DAVID enrichment score indicated on the **upper** axis. Subprocesses included in these clusters are shown in darker colors and their fold-change indicated at the **lower** axis of the graph. **B**, Relative expression of selected genes from Cluster 1 shown in **A** that were specifically expressed in brain but not peripheral ECs according to Hupe et al.[30] Twenty genes were downregulated. Twelve of these genes were transmembrane transporters or coreceptors and 8 belong to the family of ECM proteins expressed ≈20-fold higher in brain ECs compared with ECs from other organs (Table VII in the online-only Data Supplement). n=3. **C**, A significant repression of 8 genes, 50% and 84%, were observed (FDR<0.001) in *Axin1*$^{iEC-OE}$ mice at E11.5. **D** and **E**, Staining of flatmounted forebrain tissues of control and *Axin1*$^{iEC-OE}$ embryos at E11.5 with antibodies recognizing CD31-expressing ECs (green) and either apolipoprotein D (APOD; **D**) or serine protease HTRA3 (HTRA3; **E**), shown in red. **F**, Quantification of the abundance of APOD or HTRA3 measured as percent of red pixels from the experiment in **D** and **E**. n=4 mice per group. *P<0.05. **G**, Temporal expression profile in brain ECs during blood-brain barrier (BBB) formation and maturation displayed clustering in 2 families, one exhibiting increasing expression from E11.5 to E17.5, or plateauing expression after initial BBB-maturation at E15.5, and another showing increasing expression that peaked at BBB-maturation stages (E14.5/E15.5) followed by reduced expression at later developmental stages (**H**). Among downregulated genes in **G**, 4 genes, *Adamtsl2*, *Htra3*, *Spock2*, and *Wfdc1*, were all significantly downregulated also in *Axin1*$^{iEC-OE}$ mouse embryos at E14.5 and in *Ctnnb1-KO*^{iEC}, at E14.5 compared with littermate controls, 2 d after Cre-induction. Fold-change is indicated on the lower axis. Dark bars indicate genes significantly deregulated (FDR<0.05). The RPKM values of each gene is indicated in parenthesis for the *Axin1*$^{iEC-OE}$ mice or controls (wt) at E11.5.

elevated mRNA level seen at E11.5 in these mice might be a compensation mechanism. Combined, these results indicate that AOE and concomitant suppression of β-catenin signaling results in transcriptional changes involved in BBB formation and maturation that precede vascular leakiness and rupture. Moreover, our data indicate that inhibition of Wnt-signaling does not affect EC specification per se but impairs the acquisition of CNS EC-specific phenotypes.

To investigate the functional outcomes associated with deregulated gene expression in *Axin1*$^{iEC-OE}$ mice, we performed a pathway analysis including all 583 upregulated or downregulated genes, using DAVID.[51] Using stringent criteria (false discovery rate [FDR]<0.1), 3 significantly enriched functional gene clusters were identified; extracellular proteins, chemokine signaling, and metal-binding proteins, of which the extracellular proteins cluster was the most significant and contained the most deregulated genes (Figure 7A). The ECM is important for coordinating brain vascular development, remodeling, and BBB maturation,[27] and we confirmed that nonforebrain CNS vessels, as well as peripheral vasculatures in the paw and dorsal intersegmental region, were not affected by 2 days of AOE in E11.5 *Axin1*$^{iEC-OE}$ mice compared with controls (Figure V in the online-only Data Supplement), suggesting that forebrain vessels were selectively affected in these mice. We, therefore, used our recently released resource[30] to filter the cluster of deregulated extracellular proteins for genes specifically expressed in brain ECs but not in ECs from other tissues or in non-EC brain cells, resulting in a list of 20 genes, all of which were downregulated (Table VII in the online-only Data Supplement). Twelve of these genes were transmembrane transporters or coreceptors and 8 (*Adamtsl2* [ADAMTS-like protein 2], *Apod* [apolipoprotein D], *Ctsw* [Cathepsin W], *Htra3* [serine protease HTRA3], *Pglyrp1* [peptidoglycan recognition protein 1], *Spock2* [Testican-2], *Ttyh2* [protein tweety homolog 2], and *Wfdc1* [WAP four-disulfide core domain protein 1]) belong to the family of bona fide ECM proteins expressed on average 20-fold higher in brain ECs compared with ECs from other tissues (Figure 7B). These 8 genes were significantly repressed (FDR<0.001) by 50% to 84% in *Axin1*$^{iEC-OE}$ mice at E11.5 (Figure 7C). We validated that the expression of 3 representative genes among these 8, *Apod*, *Htra3*, and *Adamtsl2* were indeed reduced by investigating the abundance of their protein products apolipoprotein D, serine protease HTRA3, and ADAMTS-like protein 2 using immunostaining (Figure 7D and 7E; Figure VIB in the online-only Data Supplement), although this trend did not reach significance in the apolipoprotein D group (Figure 7F), likely because of the large intergroup variation. Using in situ hybridization, Adamtsl2 mRNA was confirmed to be expressed exclusively in the forebrain vasculature (Figure VIA in the online-only Data Supplement). To investigate the potential role of these genes during BBB formation and maturation, we next investigated their temporal expression pattern in brain ECs during development. The genes clustered in 2 families, one exhibiting increasing expression from E11.5 to E17.5, or plateauing expression after initial BBB-maturation at E15.5, and another exhibiting increasing expression that peaked at BBB-maturation stages (E14.5/E15.5) followed by a decrease in expression at later developmental stages (Figure 7G). These expression patterns coincide with the development and initial maturation of the BBB are consistent with genes important for generating and maintaining BBB characteristics during embryonic development. To further substantiate this hypothesis, we investigated if these genes were also repressed in both *Axin1*$^{iEC-OE}$ and *Ctnnb1-KO*^{iEC} mice at E14.5, corresponding to a point in development where robust BBB characteristics are observed in the CNS vasculature in control mice. We found that transcripts of 4 genes, *Adamtsl2*, *Htra3*, *Spock2*, and *Wfdc1*, were all significantly downregulated at this later developmental time point in both of these 2 other mouse models (Figure 7H). That Apod mRNA levels were only reduced transiently at E11.5 but not E14.5 may explain why we failed to observe a robust downregulation of this factor at the protein level. All but one (Spock2) of the 4 persistently downregulated transcripts have not been previously described as Wnt-β-catenin targets and are, therefore, novel downstream potential regulators of β-catenin functions in CNS vessels. While these factors are downregulated at both mRNA (Figure 7H) and protein levels (Figure 7E and 7F; Figure VIB in the online-only Data Supplement), the regulation of other widely expressed EC-produced ECM proteins, such as Collagen IV (Figure 2I) or Laminin-α4 remain unchanged (Figure 2W). This suggests that Adamtsl2, Htra3, Spock2, and Wfdc1 establish a β-catenin–induced vascular ECM signature that is niche specific to the forebrain and required for vascular stabilization in this region. To analyze whether pathological vascular destabilization and hemorrhage in the forebrain

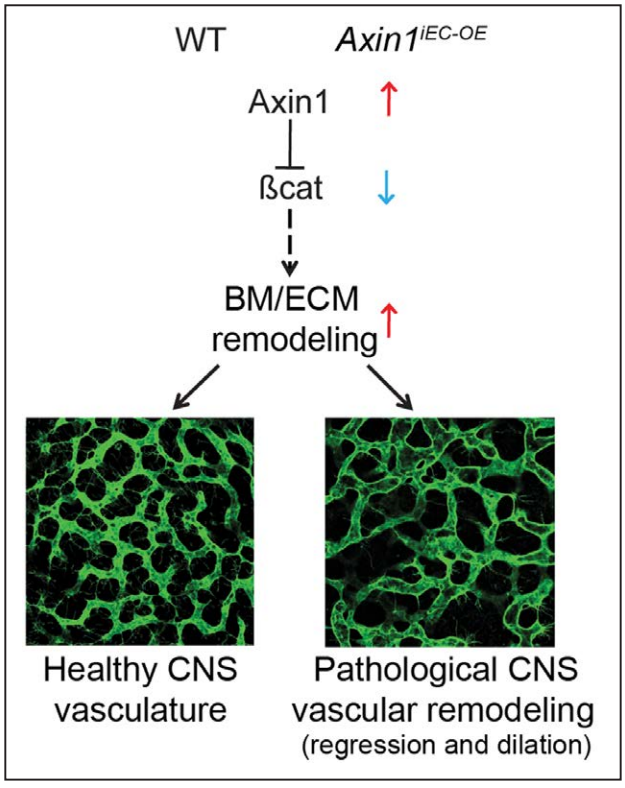

Figure 8. Illustration of the proposed pathway involved in β-catenin–induced blood-brain barrier (BBB)-development in mice. Axin1-mediated suppression of β-catenin (β-cat) signaling in *Axin1*$^{iEC-OE}$ (Cdh5ERT2;Cre;R26Axin1IL^{het}) mice leads to basement membrane (BM)/ECM (extracellular matrix) remodeling, which in turn disrupts central nervous system (CNS) vascular development by inducing vascular regression, dilation and eventually BBB failure and cerebral hemorrhage.

of *Axin1*$^{iEC-OE}$ and *Ctnnb1*-KO^{iEC} mice could be ascribed to a single of these genes, we tested this focusing on the gene exhibiting the highest basal expression at E11.5, *Adamtsl2*, as we hypothesized that high levels of this protein might, therefore, be important for maintaining the vascular stability and barrier characteristics during development. No forebrain hemorrhage was observed in *Adamtsl2*-KO mice at E14.5 (Figure VIC in the online-only Data Supplement), nor was *Adamtsl2* overexpression able to rescue the pathological brain vascular phenotypes observed in *Axin1*$^{iEC-OE}$ zebrafish larvae at 60 hpf (Figure VII in the online-only Data Supplement), suggesting that Adamtsl2 (or likely any other of these factors) does not act alone but rather that β-catenin signaling is important for a coordinated expression of this panel of ECM factors which act in concert to promote BBB formation and maintenance during development (Figure 8).

Taken together, the data presented strongly indicate that AOE-induced suppression of β-catenin signaling leads to impaired production of forebrain-specific, vascular ECM proteins, which drives initial vascular regression and subsequent vascular dilation, barrier disruption and eventually hemorrhage, specifically in the forebrain.

Discussion

Elimination of the neuroepithelium derived Wnt ligands, Wnt*7a* and Wnt*7b* implicated the Wnt/β-catenin pathway as a key player in formation and differentiation of the CNS vasculature.[6–8,52] Interestingly, the CNS-specific vascular phenotype in the *Axin1*$^{iEC-OE}$ mutant described here, exhibiting ventral forebrain hemorrhage, Slc2a1/Glut1 downregulation but lack of pericyte and radial glia defects, can also be found in the CNS of endothelial-specific Wnt7a and –b coreceptor GPR124 mutant mice.[20–22] Moreover, Wnt7a/7b-Gpr124/Reck-signaling was recently found to be required for CNS tip cell functions in zebrafish indicating that reduced Wnt/β-catenin could lead to reduced CNS vascular sprouting.[25]

In this study, we found that impaired Wnt/β-catenin activity in ECs because of overexpression of Axin1 in mice is associated with immediate regression of newly formed CNS sprouts and vessels in the forebrain. Contrary to the reported blockade of vessel sprouting into the CNS when endothelial β-catenin signaling was inhibited at earlier developmental stages,[25] we found that vascular tip cell formation and sprouting was not impaired on EC-specific AOE or β-catenin ablation at postvascular invasion stages when vessels were already present in the CNS, suggesting that β-catenin plays different roles in the ECs initially invading into the CNS compared with those that are expanding within the CNS. Regardless of the developmental window targeted after perineural vascular plexus formation, 4 days of induced endothelial AOE was required to produce significantly compromised BBB-integrity leading to hemorrhage, suggesting that β-catenin signaling is equally important for maintaining CNS vascular integrity throughout development. Notably, vascular barrier dysfunction examined by 70 kDa dextran injection at a time point after detectable vascular pathology but preceding the onset of hemorrhage exhibited no detectable tracer leakage in *Axin1*$^{iEC-OE}$ embryonic forebrains, in line with a previous report where no 70 kDa dextran leakage was found in cerebral vascular dysplasic *Itgb8* mutant embryonic brain one day before (E11.5) the eventual hemorrhage (E12.5). However, pericyte deficient *Pdgfb*$^{ret/ret}$[47,48,53] positive controls displayed a robust leakage, severely disrupted BBB but no obvious hemorrhage and comparatively normal vascular morphogenesis.[46] As smaller tracers spontaneously leak at stages before E14.5,[45] we used a larger molecule that is restricted to the forebrain vasculature under physiological conditions at this stage. For this reason, we cannot rule out that smaller tracers of molecular weight <70 kDa might leak more readily in *Axin1*$^{iEC-OE}$ compared to control littermates; it is thus possible that *Axin1*$^{iEC-OE}$ mice exhibit increased BBB-leakage of <70 kDa molecules. This issue requires further analysis using a range of differently sized tracers.

Interestingly, we found that *Axin1*$^{iEC-OE}$ led to specific BBB-disruption in the forebrain and did not affect non-CNS vasculatures, BBB-integrity or morphogenesis of other CNS vasculatures, including that in the spinal cord, which is also disrupted upon EC-specific β-catenin ablation.[6] We propose that the reason for the specific sensitivity of forebrain vasculature in responce to AOE is that vessels in the forebrain require a particularly high level of β-catenin signaling to maintain stability, whereas lower levels in other CNS vasculature may trigger a stronger compensation by alternative γ-catenin–mediated signaling.[6] This hypothesis is supported by the finding that β-catenin signaling was not completely shut off in our *Axin1*$^{iEC-OE}$ mouse model, and ≈40% of endogenous reporter activity and 20% to 40% expression of downstream target genes were retained 2 days after AOE. This may be sufficient to protect the BBB in other CNS tissues but not in the forebrain. Indeed, Axin1 is known to be a modulator, involved in fine-tuning of β-catenin–signaling levels rather than a binary on/off switch,[54] which is consistent with the data reported here. As such, our findings suggest that β-catenin signaling may be required at varying levels in distinct CNS compartments during development, and imply that targeting β-catenin signaling genetically or pharmacologically may lead to phenotypes in the forebrain vasculature even at low levels of inhibition, before phenotypes are observed in other CNS vascular beds.

Mechanistically, we reveal that reduced Wnt/β-catenin signaling led to the repression of 8 CNS EC-specific ECM genes that under normal development were robustly expressed in CNS ECs but not by ECs of other organs.[30] This suggests that these genes are important for β-catenin–mediated BBB formation/maintenance, and that this is occurring by regulation of multiple genes acting in parallel. Six of the proteins encoded by these genes, *Adamtsl2, Apod, Pglyrp, Spock2, Ttyh2*, and *Wfdc1*, are ECM-associated proteins of which only Apod and Spock2 have previously been implicated in regulation of BBB development and function,[55–57] and 2, Ctsw and Htra3 are ECM modulating proteases, with no previously described role in BBB regulation. The expression of these genes, however, strongly coincided with BBB development and maturation; their expression increased between E11.5 and E14.5/E15.5, when the first BBB functions have become robust throughout the CNS, followed by either plateaued or decreased expression at later developmental stages. Furthermore, 4 of these factors, Adamtsl2, Htra3, Spock2, and Wfdc1, were also robustly and significantly downregulated in both *Axin1*$^{iEC-OE}$ and EC-specific β-catenin-KO embryos at

E14.5, both suffering from impaired BBB development, and Adamtsl2 and Htra3 were further found to be downregulated also at the protein level already at E11.5 consistent with an important role for these factors in this process. Of these, only Testican-2, encoded by Spock2 has previously been linked to BBB formation[49,55–57] and breakdown associated with astrocytoma progression[58] and none of these genes have previously been associated with Wnt-β-catenin signaling. Nevertheless, the data presented here, coupled to our recently published resource of genes specifically expressed in brain ECs but not peripheral ECs during development, strongly imply that these 4 genes may play important roles downstream of Wnt-β–catenin during BBB development and maintenance, an issue that should be specifically addressed in future studies. It is, however, likely that all of these factors act in concert, possibly together with other ECM factors and proteases, to mediate the Wnt-β–catenin effects on the BBB and that this is not entirely dependent on any single one of these. This is supported by our findings, demonstrating a lack of forebrain hemorrhage in *Adamtsl2*-KO mice and the inability of *Adamtsl2* overexpression to rescue Axin1-induced vascular regression in the CNS during zebrafish development. As such, these findings implicate β-catenin signaling as a central orchestrator of ECM formation and remodeling during BBB formation and maintenance, respectively, and suggests that a complex deregulation of ECM may be, at least in part, responsible for the CNS vascular defects observed in the *Axin1*$^{iEC-OE}$ and EC-specific β–catenin-knockout mice and zebrafish.

Interestingly, phenotypes such as vessel regression without widespread defects in pericyte recruitment, that we found in our *Axin1*$^{iEC-OE}$ mice and zebrafish, closely resemble the vascular phenotype of induced endothelial-specific TGFβR2 (transforming growth factor, beta receptor II) deletion.[59] In Smad2/3 double knockout mouse embryos[60] and in TGFβ1 (transforming growth factor beta 1), TGFβR2, and integrin αVb8 loss-of-function mouse embryos,[46] hemorrhage of the forebrain specifically was observed at E12.5 and E11.5, respectively, but the extent of hemorrhage was stronger in the Smad2/3 knockout strain.[61] TGFβ signaling is primarily induced by its release from the ECM, a process regulated by several of the ECM genes found to be repressed in both EC-specific β-catenin-knockout and *Axin1*$^{iEC-OE}$ mice[27] suggesting that the β-catenin and TGFβ pathways could be functionally coupled during CNS vascular development in mice.[36,58,62,63]

In conclusion, the results presented here strongly suggest that suppression of β-catenin signaling by EC-specific AOE leads to regression, subsequent dilation, and pathological remodeling of (fore)brain vessels eventually culminating in BBB-breakdown and cerebral hemorrhage. This is likely because of a deregulation of forebrain EC-specific ECM proteins and remodeling factors, leading to disrupted ECM formation and maintenance at the BBB-niche in the brain of *Axin1*$^{iEC-OE}$mice.

Acknowledgments

We thank Dr Christian Göritz for providing reagents and animal housing, Dr Olov Andersson for providing reagents and equipment for pilot experiments, Drs Lars Jakobsson and Maarja Andaloussi Mäe/Professor Christer Betsholtz for providing antibodies, Dr Kirsty Spalding for granting access to FACS and related equipment during pilot studies, Dr Douglas W. Houston (University of Iowa) for kindly providing the FLAG-axin1/pCS2+ construct, Dr Jan Mulder and Professor Peter Nilsson at SciLife Lab for input regarding antibodies from the Human Protein Atlas, Mattias Karlén for kindly improving our illustrations and Dr Igor Adameyko and Professor Thomas Perlmann for comments on the article.

Sources of Funding

This work was partly supported by Cancerfonden [CAN 2010/679]. B. Hot was funded by Karolinska Funding for Doctorial Studies. L.D.E. Jensen was financially supported by the Swedish Society for Medical Research, Jeanssons Stiftelser, the Swedish Research Council and H2020-MSCA-RISE (3D-NEONET). D. Ramsköld was funded by Johnson & Johnson (K240001043). V.M. Lauschke was supported by a Marie Curie FP7 people initiative Fellowship (626544), D. Hubmacher by National Institutes of Health (AR070748), S.S. Apte by National Institutes of Health (AR53890), and D. Nyqvist by the Swedish Society for Medical Research and the Swedish Research Council. J.M. Stenman was supported by Wenner-Gren Fellows and J. Kele was funded by Swedish Society for Medical Research, Swedish Brain Foundation, Tore Nilsons Stiftelse, Tornspiran, Lars Hiertas Stiftelse, Jane and Dan Olsson Foundations, Samariten and Bergvalls Stiftelse.

Disclosures

None.

References

1. Zhao Z, Nelson AR, Betsholtz C, Zlokovic BV. Establishment and dysfunction of the blood-brain barrier. *Cell.* 2015;163:1064–1078. doi: 10.1016/j.cell.2015.10.067
2. Engelhardt B, Liebner S. Novel insights into the development and maintenance of the blood-brain barrier. *Cell Tissue Res.* 2014;355:687–699. doi: 10.1007/s00441-014-1811-2
3. Thomsen MS, Routhe LJ, Moos T. The vascular basement membrane in the healthy and pathological brain. *J Cereb Blood Flow Metab.* 2017;37:3300–3317. doi: 10.1177/0271678X17722436
4. Hogan KA, Ambler CA, Chapman DL, Bautch VL. The neural tube patterns vessels developmentally using the VEGF signaling pathway. *Development.* 2004;131:1503–1513. doi: 10.1242/dev.01039
5. Engelhardt B. Development of the blood-brain barrier. *Cell Tissue Res.* 2003;314:119–129. doi: 10.1007/s00441-003-0751-z
6. Stenman JM, Rajagopal J, Carroll TJ, Ishibashi M, McMahon J, McMahon AP. Canonical Wnt signaling regulates organ-specific assembly and differentiation of CNS vasculature. *Science.* 2008;322:1247–1250. doi: 10.1126/science.1164594
7. Liebner S, Corada M, Bangsow T, Babbage J, Taddei A, Czupalla CJ, Reis M, Felici A, Wolburg H, Fruttiger M, Taketo MM, von Melchner H, Plate KH, Gerhardt H, Dejana E. Wnt/beta-catenin signaling controls development of the blood-brain barrier. *J Cell Biol.* 2008;183:409–417. doi: 10.1083/jcb.200806024
8. Daneman R, Agalliu D, Zhou L, Kuhnert F, Kuo CJ, Barres BA. Wnt/beta-catenin signaling is required for CNS, but not non-CNS, angiogenesis. *Proc Natl Acad Sci USA.* 2009;106:641–646.
9. Zhou Y, Wang Y, Tischfield M, Williams J, Smallwood PM, Rattner A, Taketo MM, Nathans J. Canonical WNT signaling components in vascular development and barrier formation. *J Clin Invest.* 2014;124:3825–3846. doi: 10.1172/JCI76431
10. Wang Y, Rattner A, Zhou Y, Williams J, Smallwood PM, Nathans J. Norrin/Frizzled4 signaling in retinal vascular development and blood brain barrier plasticity. *Cell.* 2012;151:1332–1344. doi: 10.1016/j.cell.2012.10.042
11. Moro E, Ozhan-Kizil G, Mongera A, Beis D, Wierzbicki C, Young RM, Bournele D, Domenichini A, Valdivia LE, Lum L, Chen C, Amatruda JF, Tiso N, Weidinger G, Argenton F. *In vivo* Wnt signaling tracing through a transgenic biosensor fish reveals novel activity domains. *Dev Biol.* 2012;366:327–340. doi: 10.1016/j.ydbio.2012.03.023
12. Ma S, Kwon HJ, Johng H, Zang K, Huang Z. Radial glial neural progenitors regulate nascent brain vascular network stabilization via inhibition of Wnt signaling. *PLoS Biol.* 2013;11:e1001469. doi: 10.1371/journal.pbio.1001469
13. Valenta T, Gay M, Steiner S, Draganova K, Zemke M, Hoffmans R, Cinelli P, Aguet M, Sommer L, Basler K. Probing

transcription-specific outputs of β-catenin in vivo. *Genes Dev.* 2011;25:2631–2643. doi: 10.1101/gad.181289.111
14. Nelson WJ, Nusse R. Convergence of Wnt, beta-catenin, and cadherin pathways. *Science.* 2004;303:1483–1487. doi: 10.1126/science.1094291
15. Zeng L, Fagotto F, Zhang T, Hsu W, Vasicek TJ, Perry WL III, Lee JJ, Tilghman SM, Gumbiner BM, Costantini F. The mouse Fused locus encodes Axin, an inhibitor of the Wnt signaling pathway that regulates embryonic axis formation. *Cell.* 1997;90:181–192.
16. Xu Q, Wang Y, Dabdoub A, Smallwood PM, Williams J, Woods C, Kelley MW, Jiang L, Tasman W, Zhang K, Nathans J. Vascular development in the retina and inner ear: control by Norrin and Frizzled-4, a high-affinity ligand-receptor pair. *Cell.* 2004;116:883–895.
17. Ye X, Wang Y, Cahill H, Yu M, Badea TC, Smallwood PM, Peachey NS, Nathans J. Norrin, frizzled-4, and Lrp5 signaling in endothelial cells controls a genetic program for retinal vascularization. *Cell.* 2009;139:285–298. doi: 10.1016/j.cell.2009.07.047
18. Paes KT, Wang E, Henze K, Vogel P, Read R, Suwanichkul A, Kirkpatrick LL, Potter D, Newhouse MM, Rice DS. Frizzled 4 is required for retinal angiogenesis and maintenance of the blood-retina barrier. *Invest Ophthalmol Vis Sci.* 2011;52:6452–6461. doi: 10.1167/iovs.10-7146
19. Junge HJ, Yang S, Burton JB, Paes K, Shu X, French DM, Costa M, Rice DS, Ye W. TSPAN12 regulates retinal vascular development by promoting Norrin- but not Wnt-induced FZD4/beta-catenin signaling. *Cell.* 2009;139:299–311. doi: 10.1016/j.cell.2009.07.048
20. Kuhnert F, Mancuso MR, Shamloo A, Wang HT, Choksi V, Florek M, Su H, Fruttiger M, Young WL, Heilshorn SC, Kuo CJ. Essential regulation of CNS angiogenesis by the orphan G protein-coupled receptor GPR124. *Science.* 2010;330:985–989. doi: 10.1126/science.1196554
21. Cullen M, Elzarrad MK, Seaman S, et al. GPR124, an orphan G protein-coupled receptor, is required for CNS-specific vascularization and establishment of the blood-brain barrier. *Proc Natl Acad Sci USA.* 2011;108:5759–5764.
22. Anderson KD, Pan L, Yang XM, et al. Angiogenic sprouting into neural tissue requires Gpr124, an orphan G protein-coupled receptor. *Proc Natl Acad Sci USA*. 2011;108:2807–2812.
23. Eubelen M, Bostaille N, Cabochette P, et al. A molecular mechanism for Wnt ligand-specific signaling. *Science*. 2018;361:eaat1178.
24. Chandana EP, Maeda Y, Ueda A, et al. Involvement of the reck tumor suppressor protein in maternal and embryonic vascular remodeling in mice. *BMC Dev Biol.* 2010;10:84. doi: 10.1186/1471-213X-10-84
25. Vanhollebeke B, Stone OA, Bostaille N, et al. Tip cell-specific requirement for an atypical Gpr124- and Reck-dependent Wnt/beta-catenin pathway during brain angiogenesis. *Elife*. 2015;4:e06489.
26. Ding JY, Kreipke CW, Schafer P, Schafer S, Speirs SL, Rafols JA. Synapse loss regulated by matrix metalloproteinases in traumatic brain injury is associated with hypoxia inducible factor-1alpha expression. *Brain Res.* 2009;1268:125–134. doi: 10.1016/j.brainres.2009.02.060
27. Baeten KM, Akassoglou K. Extracellular matrix and matrix receptors in blood-brain barrier formation and stroke. *Dev Neurobiol.* 2011;71:1018–1039. doi: 10.1002/dneu.20954
28. Menezes MJ, McClenahan FK, Leiton CV, Aranmolate A, Shan X, Colognato H. The extracellular matrix protein laminin α2 regulates the maturation and function of the blood-brain barrier. *J Neurosci.* 2014;34:15260–15280. doi: 10.1523/JNEUROSCI.3678-13.2014
29. Ramsköld D, Luo S, Wang YC, Li R, Deng Q, Faridani OR, Daniels GA, Khrebtukova I, Loring JF, Laurent LC, Schroth GP, Sandberg R. Full-length mRNA-Seq from single-cell levels of RNA and individual circulating tumor cells. *Nat Biotechnol.* 2012;30:777–782. doi: 10.1038/nbt.2282
30. Hupe M, Li MX, Kneitz S, Davydova D, Yokota C, Kele J, Hot B, Stenman JM, Gessler M. Gene expression profiles of brain endothelial cells during embryonic development at bulk and single-cell levels. *Sci Signal*. 2017;10:eaag2476.
31. Hupe M, Li MX, Gertow Gillner K, Adams RH, Stenman JM. Evaluation of TRAP-sequencing technology with a versatile conditional mouse model. *Nucleic Acids Res.* 2014;42:e14. doi: 10.1093/nar/gkt995
32. Sörensen I, Adams RH, Gossler A. DLL1-mediated Notch activation regulates endothelial identity in mouse fetal arteries. *Blood.* 2009;113:5680–5688. doi: 10.1182/blood-2008-08-174508
33. Motoike T, Markham DW, Rossant J, Sato TN. Evidence for novel fate of Flk1+ progenitor: contribution to muscle lineage. *Genesis.* 2003;35:153–159. doi: 10.1002/gene.10175
34. Brault V, Moore R, Kutsch S, Ishibashi M, Rowitch DH, McMahon AP, Sommer L, Boussadia O, Kemler R. Inactivation of the beta-catenin gene by Wnt1-Cre-mediated deletion results in dramatic brain malformation and failure of craniofacial development. *Development.* 2001;128:1253–1264.
35. Ferrer-Vaquer A, Piliszek A, Tian G, Aho RJ, Dufort D, Hadjantonakis AK. A sensitive and bright single-cell resolution live imaging reporter of Wnt/β-catenin signaling in the mouse. *BMC Dev Biol.* 2010;10:121. doi: 10.1186/1471-213X-10-121
36. Hubmacher D, Wang LW, Mecham RP, Reinhardt DP, Apte SS. Adamtsl2 deletion results in bronchial fibrillin microfibril accumulation and bronchial epithelial dysplasia–a novel mouse model providing insights into geleophysic dysplasia. *Dis Model Mech.* 2015;8:487–499. doi: 10.1242/dmm.017046
37. Mao J, Barrow J, McMahon J, Vaughan J, McMahon AP. An ES cell system for rapid, spatial and temporal analysis of gene function *in vitro* and in vivo. *Nucleic Acids Res.* 2005;33:e155. doi: 10.1093/nar/gni146
38. Eggan K, Akutsu H, Loring J, Jackson-Grusby L, Klemm M, Rideout WM III, Yanagimachi R, Jaenisch R. Hybrid vigor, fetal overgrowth, and viability of mice derived by nuclear cloning and tetraploid embryo complementation. *Proc Natl Acad Sci USA*. 2001;98:6209–6214.
39. Schindelin J, Arganda-Carreras I, Frise E, et al. Fiji: an open-source platform for biological-image analysis. *Nat Methods.* 2012;9:676–682. doi: 10.1038/nmeth.2019
40. Langmead B, Trapnell C, Pop M, Salzberg SL. Ultrafast and memory-efficient alignment of short DNA sequences to the human genome. *Genome Biol.* 2009;10:R25. doi: 10.1186/gb-2009-10-3-r25
41. Ramsköld D, Wang ET, Burge CB, Sandberg R. An abundance of ubiquitously expressed genes revealed by tissue transcriptome sequence data. *PLoS Comput Biol.* 2009;5:e1000598. doi: 10.1371/journal.pcbi.1000598
42. Beis D, Bartman T, Jin SW, et al. Genetic and cellular analyses of zebrafish atrioventricular cushion and valve development. *Development.* 2005;132:4193–4204. doi: 10.1242/dev.01970
43. Chi NC, Shaw RM, De Val S, Kang G, Jan LY, Black BL, Stainier DY. Foxn4 directly regulates tbx2b expression and atrioventricular canal formation. *Genes Dev.* 2008;22:734–739. doi: 10.1101/gad.1629408
44. Kagermeier-Schenk B, Wehner D, Ozhan-Kizil G, Yamamoto H, Li J, Kirchner K, Hoffmann C, Stern P, Kikuchi A, Schambony A, Weidinger G. Waif1/5T4 inhibits Wnt/β-catenin signaling and activates noncanonical Wnt pathways by modifying LRP6 subcellular localization. *Dev Cell.* 2011;21:1129–1143. doi: 10.1016/j.devcel.2011.10.015
45. Ben-Zvi A, Lacoste B, Kur E, Andreone BJ, Mayshar Y, Yan H, Gu C. Mfsd2a is critical for the formation and function of the blood-brain barrier. *Nature.* 2014;509:507–511. doi: 10.1038/nature13324
46. Arnold TD, Niaudet C, Pang MF, Siegenthaler J, Gaengel K, Jung B, Ferrero GM, Mukouyama YS, Fuxe J, Akhurst R, Betsholtz C, Sheppard D, Reichardt LF. Excessive vascular sprouting underlies cerebral hemorrhage in mice lacking αVβ8-TGFβ signaling in the brain. *Development.* 2014;141:4489–4499. doi: 10.1242/dev.107193
47. Armulik A, Genové G, Mäe M, Nisancioglu MH, Wallgard E, Niaudet C, He L, Norlin J, Lindblom P, Strittmatter K, Johansson BR, Betsholtz C. Pericytes regulate the blood-brain barrier. *Nature.* 2010;468:557–561. doi: 10.1038/nature09522
48. Daneman R, Zhou L, Kebede AA, Barres BA. Pericytes are required for blood-brain barrier integrity during embryogenesis. *Nature.* 2010;468:562–566. doi: 10.1038/nature09513
49. Daneman R, Zhou L, Agalliu D, Cahoy JD, Kaushal A, Barres BA. The mouse blood-brain barrier transcriptome: a new resource for understanding the development and function of brain endothelial cells. *PLoS One.* 2010;5:e13741. doi: 10.1371/journal.pone.0013741
50. Nitta T, Hata M, Gotoh S, Seo Y, Sasaki H, Hashimoto N, Furuse M, Tsukita S. Size-selective loosening of the blood-brain barrier in claudin-5-deficient mice. *J Cell Biol.* 2003;161:653–660. doi: 10.1083/jcb.200302070
51. Huang DW, Sherman BT, Tan Q, Collins JR, Alvord WG, Roayaei J, Stephens R, Baseler MW, Lane HC, Lempicki RA. The DAVID gene functional classification tool: a novel biological module-centric algorithm to functionally analyze large gene lists. *Genome Biol.* 2007;8:R183. doi: 10.1186/gb-2007-8-9-r183
52. Parr BA, Shea MJ, Vassileva G, McMahon AP. Mouse Wnt genes exhibit discrete domains of expression in the early embryonic CNS and limb buds. *Development.* 1993;119:247–261.
53. Bell RD, Winkler EA, Sagare AP, Singh I, LaRue B, Deane R, Zlokovic BV. Pericytes control key neurovascular functions and neuronal phenotype in the adult brain and during brain aging. *Neuron.* 2010;68:409–427. doi: 10.1016/j.neuron.2010.09.043
54. Song X, Wang S, Li L. New insights into the regulation of Axin function in canonical Wnt signaling pathway. *Protein Cell.* 2014;5:186–193. doi: 10.1007/s13238-014-0019-2
55. Rickhag M, Deierborg T, Patel S, Ruscher K, Wieloch T. Apolipoprotein D is elevated in oligodendrocytes in the peri-infarct region after experimental

stroke: influence of enriched environment. *J Cereb Blood Flow Metab.* 2008;28:551–562. doi: 10.1038/sj.jcbfm.9600552
56. Tam SJ, Richmond DL, Kaminker JS, Modrusan Z, Martin-McNulty B, Cao TC, Weimer RM, Carano RA, van Bruggen N, Watts RJ. Death receptors DR6 and TROY regulate brain vascular development. *Dev Cell.* 2012;22:403–417. doi: 10.1016/j.devcel.2011.11.018
57. Schnepp A, Komp Lindgren P, Hülsmann H, Kröger S, Paulsson M, Hartmann U. Mouse testican-2. Expression, glycosylation, and effects on neurite outgrowth. *J Biol Chem.* 2005;280:11274–11280. doi: 10.1074/jbc.M414276200
58. MacDonald TJ, Pollack IF, Okada H, Bhattacharya S, Lyons-Weiler J. Progression-associated genes in astrocytoma identified by novel microarray gene expression data reanalysis. *Methods Mol Biol*. 2007;377:203–22. doi: https://doi.org/10.1007/978-1-59745-390-5_13
59. Arnold TD, Ferrero GM, Qiu H, Phan IT, Akhurst RJ, Huang EJ, Reichardt LF. Defective retinal vascular endothelial cell development as a consequence of impaired integrin αVβ8-mediated activation of transforming growth factor-β. *J Neurosci.* 2012;32:1197–1206. doi: 10.1523/JNEUROSCI.5648-11.2012
60. Itoh F, Itoh S, Adachi T, Ichikawa K, Matsumura Y, Takagi T, Festing M, Watanabe T, Weinstein M, Karlsson S, Kato M. Smad2/Smad3 in endothelium is indispensable for vascular stability via S1PR1 and N-cadherin expressions. *Blood.* 2012;119:5320–5328. doi: 10.1182/blood-2011-12-395772
61. Nguyen HL, Lee YJ, Shin J, Lee E, Park SO, McCarty JH, Oh SP. TGF-β signaling in endothelial cells, but not neuroepithelial cells, is essential for cerebral vascular development. *Lab Invest.* 2011;91:1554–1563. doi: 10.1038/labinvest.2011.124
62. Le Goff C, Cormier-Daire V. The ADAMTS(L) family and human genetic disorders. *Hum Mol Genet.* 2011;20:R163–R167. doi: 10.1093/hmg/ddr361
63. Le Goff C, Morice-Picard F, Dagoneau N, et al. ADAMTSL2 mutations in geleophysic dysplasia demonstrate a role for ADAMTS-like proteins in TGF-beta bioavailability regulation. *Nat Genet.* 2008;40:1119–1123. doi: 10.1038/ng.199

Highlights

- Inducible Axin1 overexpression in endothelial cells impairs Wnt/β-catenin signaling and leads to hemorrhage specifically in the forebrain.
- Impaired Wnt/β-catenin signaling in endothelial cells leads to immediate vascular regression followed by dilation and disturbed expression of blood-brain barrier transporters.
- Endothelial Axin1-induced blood-brain barrier disruption does not involve reduced vascular basement membrane or mural cell coverage.
- Wnt/β-catenin signaling is required for production of endothelial cell-specific extracellular matrix signatures associated with healthy central nervous system.
- Mice that overexpress Axin specifically in endothelial cells constitute a new and powerful resource for studying downstream functional effects of reduced Wnt/β-catenin signaling and its role in blood-brain barrier regulation in health and disease.